Supporting Information

A General Strategy for Development of Single Benzene Fluorophore with Full-color-tunable, Environmentally Insensitive, and Two-photon Solid-State Emission

Zhen Xiang, [a, ‡] Zhi-Yao Wang, [a, ‡] Tian-Bing Ren, [a, ‡] Wang Xu, [a] Yu-Peng Liu, [a] Xing-Xing Zhang, [a] Peng Wu, [b] Lin Yuan [a,] * and Xiao-Bing Zhang [a]

[a]State Key Laboratory of Chemo/Biosensing and Chemometrics, College of Chemistry and Chemical Engineering, Hunan University, Changsha 410082 (PR China).

[b]Analytical & Testing Center and College of Chemistry, Sichuan University, 29 Wangjiang Road, Chengdu 610064, China

[‡]These authors contributed equally to this work.

* To whom correspondence should be addressed.

E-mail: lyuan@hnu.edu.cn.

Table of contents:

1 Experimental details

Materials and instruments. Unless otherwise stated, all reagents were purchased from commercial suppliers and used without further purification. Solvents were purified by standard methods prior to use. Twice-distilled water was used throughout all experiments. Mass spectrometry (MS) analyses were conducted on a Finnigan MAT 95 XP spectrometer. NMR spectra were recorded on Bruker-400, using TMS as the internal standard. Electronic absorption spectra were obtained on a LabTech UV Power spectrometer. One-photon photoluminescence spectra were recorded on a HITACHI F4600/F7000 fluorescence spectrophotometer with a 1 cm standard quartz cell. Two-photon excited fluorescence emission was measured under the excitation of a mode-locked Ti: sapphire femtosecond pulsed laser (Chameleon Ultra I, Coherent Inc.). Two-photon solids imaging were performed on an Olympus FV1000 multi-photon laser scanning con-focal microscope equipped with a CCD camera. TLC analysis was performed on silica gel plates and column chromatography was conducted over silica gel (mesh 100–200) columns, obtained from the Yantai Jiangyou silica gel Development Company Limited.

Calculation of fluorescence quantum yield. Fluorescence quantum yield was determined using optically matching solutions of Quinine sulfate (Φ_f = 0.54 in 0.1 M H_2SO_4 solution)[1], rhodamine 6G (Φ_f = 0.95 in ethanol)[2] and cresol purple (Φ_f = 0.58 in ethanol)[3] as the standard and the quantum yield was calculated using the following equation:

$$\Phi_s = \Phi_r(A_rF_s/A_sF_r)\ (n_s/n_r)^2$$

where, s and r denote sample and reference, respectively. A is the absorbance. F is the relative integrated fluorescence intensity and n is the refractive index of the solvent.

Measurement of two-photon cross section. The two-photon cross section (σ) was determined by using a femtosecond (fs) fluorescence measurement technique. Two-photon cross sections of **SB-Fluor** solution were measured in CH_2Cl_2 and 25 mM PBS buffer (pH 7.4), at the concentration of 10.0×10^{-6} M. Two-photon cross sections of solid **SB-Fluor** were estimated with the quantum dots of **SB-Fluor** by PEG-PPG-PEG14600 encapsulation, at the concentration of 10.0×10^{-6} M in water.

The two-photon fluorescence intensity was measured at 710-850 nm by using Rhodamine B in MeOH as the standard. The two-photon property of Rhodamine B has been well characterized in the literature.[4] The two-photon cross-section was calculated by using $\sigma_s = \sigma_r(F_s n_s^2 \Phi_r C_r)/(F_r n_r^2 \Phi_s C_s)$, where the subscripts s and r stand for the sample and reference molecules. F is the average fluorescence intensity; n is the refractive index of the solvent; C is the concentration; Φ is the quantum yield; and σ_r is the two-photon cross-section of the reference molecule.

Computational Methods. The density functional theory calculation with B3LYP method was applied to the geometry optimization of **SB-Fluor** complex with 6-31+G(d) basis set. All geometry optimization and potential energy surface calculations were performed with the Gaussian 09 software package.

Fluorescent labelling of proteins. 1 mg of **BSA-SBF** (dissolved with 0.2 mL DMSO) and 35 mg of BSA were dissolved in 2.5 mL PBS buffer (25 mM, pH = 7.4) and left for overnight at room temperature. The **BSA-SBF** labelled BSA was recovered by passing the mixture through a SDS-polyacrylamide gel electrophoresis.

Intracellular localization of Mito-SBF and Mito-tracker Green. Images of HepG2 cells pretreated respectively with 5 μM **Mito-SBF** for 10 min and subsequently 1 μM Mito-tracker Green for 10 min. For **Mito-SBF**, λ_{ex} = 405 nm, λ_{em} = 425−475 nm; Mito-tracker Green, λ_{ex} = 488 nm, λ_{em} = 500−550 nm.

2. Supplementary Tables

Table S1. Photophysical data for SBF1-8 in CH_2Cl_2 solutions and in solids.

Comp.	λ_{Abs} /nm	$\varepsilon(M^{-1}$ $cm^{-1})$	λ_{Em} /nm	Stokes Shift/nm	Φ	λ_{Em}/nm /solid	Φ_{solid}[d]
SBF1	363	6500	432	69	0.46[a]	441	0.12
SBF2	399	5600	463	64	0.52[a]	488	0.13
SBF3	410	4800	533	123	0.50[b]	576	0.36
SBF4	431	8400	491	60	0.51[b]	528	0.16
SBF5	428	3800	543	115	0.62[b]	588	0.23
SBF6	413	3000	539	126	0.54[b]	545	0.32
SBF7	429	3400	582	153	0.06[b]	568	0.06
SBF8	505	8800	654	149	0.03[c]	n.d[e]	n.d[e]

The quantum yields were determined using [a]Quinine sulfate (Φ_f = 0.54 in 0.1 M H_2SO_4 solution), [b]rhodamine 6G (Φ_f = 0.95 in ethanol) and [c] cresol purple (Φ_f = 0.58 in ethanol) as reference. [d]Determined in an integrating sphere. [e]Under detection limit.

Table S2. Chemical structures and photo-physical properties of **SBF1-8**.

SBF1 (Solvent)	**λ_{Abs} /nm**	**$\varepsilon(M^{-1}cm^{-1})$**	**λ_{Em} /nm**	**φ**	**Stokes shift/nm**
DCM	363	6500	432	0.46	69
MeCN	366	5800	432	0.98	66
EtOH	372	6300	438	0.83	66
PBS	367	6400	443	0.49	76
SBF2 (Solvent)	**λ_{Abs} /nm**	**$\varepsilon(M^{-1}cm^{-1})$**	**λ_{Em} /nm**	**φ**	**Stokes shift/nm**
DCM	399	5600	463	0.52	64
MeCN	399	4900	478	0.58	79
EtOH	396	5200	479	0.32	83
PBS	401	4100	491	0.10	90
SBF3 (Solvent)	**λ_{Abs} /nm**	**$\varepsilon(M^{-1}cm^{-1})$**	**λ_{Em} /nm**	**φ**	**Stokes shift/nm**
DCM	410	4800	533	0.50	123
MeCN	407	4100	542	0.50	135
EtOH	407	5300	541	0.55	134
PBS	410	2900	562	0.22	153
SBF4 (Solvent)	**λ_{Abs} /nm**	**$\varepsilon(M^{-1}cm^{-1})$**	**λ_{Em} /nm**	**φ**	**Stokes shift/nm**
DCM	431	8400	491	0.51	60
MeCN	428	7800	494	0.41	66

EtOH	426	9100	495	0.53	69
PBS	421	4000	514	0.44	93
SBF5 (Solvent)	**λ_{Abs} /nm**	**$\varepsilon(M^{-1}cm^{-1})$**	**λ_{Em} /nm**	**φ**	**Stokes shift/nm**
DCM	428	3800	543	0.62	115
MeCN	422	3400	551	0.43	129
EtOH	421	4000	550	0.40	129
PBS	513	1300	566	0.17	53
SBF6 (Solvent)	**λ_{Abs} /nm**	**$\varepsilon(M^{-1}cm^{-1})$**	**λ_{Em} /nm**	**φ**	**Stokes shift/nm**
DCM	413	3000	539	0.54	126
MeCN	410	2600	544	0.55	134
EtOH	408	3200	544	0.42	136
PBS	439	3900	528	0.27	89
SBF7 (Solvent)	**λ_{Abs} /nm**	**$\varepsilon(M^{-1}cm^{-1})$**	**λ_{Em} /nm**	**φ**	**Stokes shift/nm**
DCM	429	3400	582	0.06	153
MeCN	426	4000	588	0.02	162
EtOH	430	3600	588	0.03	158
PBS	441	400	552	0.07	111
SBF8 (Solvent)	**λ_{Abs} /nm**	**$\varepsilon(M^{-1}cm^{-1})$**	**λ_{Em} /nm**	**φ**	**Stokes shift/nm**
DCM	505	8800	654	0.03	149
MeCN	519	12900	648	0.07	129
EtOH	518	9400	645	0.06	127
PBS	495	7000	645	0.02	150

Table S3. Crystal data and structure refinement for **SBF1** (CCDC 1875001).

Empirical formula	$C_8H_2F_3N_3$	
Formula weight	195.24	
Temperature	273.15 K	
Crystal system	monoclinic	
Space group	C2/c	
Unit cell dimensions	a = 7.7891(11) Å	α = 90°
	b = 9.8407(14) Å	β = 90.909(5)°
	c = 19.664(3) Å	γ = 90°
Volume	1507.0(4) $Å^3$	
Z	8	
ρ_{calc}	1.721 g/cm^3	
μ/	0.162 mm^{-1}	
F(000)	769.0	
Crystal size	0.15 × 0.14 × 0.12 mm^3	
Radiation	Mo Kα (λ = 0.71073)	
2Θ range for data collection	6.672 to 56.604°	
Index ranges	$-10 \le h \le 9$, $-13 \le k \le 13$, $-26 \le l \le 26$	
Reflections collected	7739	
Independent reflections	1882 [Rint = 0.0582, Rsigma = 0.0567]	
Data/restraints/parameters	1882/0/127	
Goodness-of-fit on F^2	1.098	
Final R indexes [I > = 2σ (I)]	R_1 = 0.0637, wR_2 = 0.1328	
Final R indexes [all data]	R_1 = 0.1052, wR_2 = 0.1512	
Largest diff. peak/hole	0.38/-0.36 e $Å^{-3}$	

Table S4. Crystal data and structure refinement for **SBF3** (CCDC 1875005).

Empirical formula	$C_{12}H_{12}F_2N_4$	
Formula weight	250.26	
Temperature	293.15 K	
Crystal system	monoclinic	
Space group	$P2_1/n$	
Unit cell dimensions	a = 12.3349(6) Å	α = 90°
	b = 7.6871(4) Å	β = 96.325(5)°
	c = 12.6994(6) Å	γ = 90°
Volume	1196.83(10) $Å^3$	
Z	4	
ρ_{calc}	1.389 g/cm^3	
μ	0.109 mm^{-1}	
F(000)	520.0	
Crystal size	0.4 × 0.4 × 0.4 mm^3	
Radiation	Mo Kα (λ = 0.71073)	
2Θ range for data collection	6.206 to 52.742°	
Index ranges	$-15 \le h \le 15$, $-6 \le k \le 9$, $-15 \le l \le 15$	
Reflections collected	4909	
Independent reflections	2446 [Rint = 0.0157, Rsigma = 0.0281]	
Data/restraints/parameters	2446/0/167	
Goodness-of-fit on F^2	1.032	
Final R indexes [I >= 2σ (I)]	R_1 = 0.0450, wR_2 = 0.1102	
Final R indexes [all data]	R_1 = 0.0669, wR_2 = 0.1243	
Largest diff. peak/hole	0.16/-0.19 e $Å^{-3}$	

3 Compound Synthesis

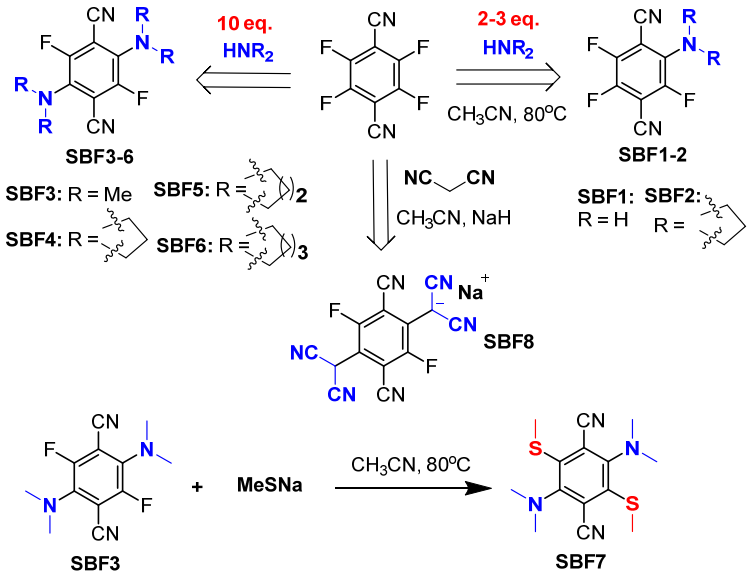

Scheme 1. The general synthetic scheme of **SBF** dyes.

SBF1: A mixture of 2,3,5,6-tetrafluoroterephthalonitrile (0.50 g, 2.50 mmol), ammonia (0.07 g, 7.50 mmol), and CH_3CN (6 mL) was stirred for 1 day at 80 °C. After cooling, the solvent was removed in a rotary evaporator and the solid obtained was purified by silica gel chromatography to get colorless powder **SBF1** (0.39 g, 80%). ^{1}H NMR (400 MHz, DMSO-d_6) δ 7.09 (s, 2H); ^{13}C NMR (100 MHz, DMSO-d_6) δ 148.3, 145.8 (dt, J = 7.1, 3.7 Hz), 138.8, 136.6 (dd, J = 15.2, 4.6 Hz), 111.1 (t, J = 3.5 Hz), 109.0 (d, J = 3.8 Hz), 97.1, 89.8; ^{19}F NMR (376 MHz, DMSO-d_6) δ -126.90 (dd, J = 12.6, 9.0 Hz, 1F), -136.37 (dd, J = 21.8, 12.6 Hz, 1F), -151.08 (dd, J = 21.8, 9.0 Hz, 1F). MS (EI): calcd for $C_8H_2F_3N_3$ 197.0, found 197.1.

SBF2: A mixture of 2,3,5,6-tetrafluoroterephthalonitrile (0.50 g, 2.50 mmol), azetidine (0.28 g, 5.0 mmol), and CH_3CN (6 mL) was stirred for 10 h at 80 °C. After cooling, the solvent was removed in a rotary evaporator and the solid obtained was purified by silica gel chromatography to get light yellow powder **SBF2** (0.48 g, 82%). ^{1}H NMR (400 MHz, $CDCl_3$) δ 4.46 (t, J = 7.4 Hz, 4H), 2.50 – 2.33 (m, 2H); ^{13}C NMR (100 MHz, $CDCl_3$) δ 148.5, 145.5, 137.4, 111.0, 106.5, 105.9, 97.9, 89.9, 55.8, 17.8; ^{19}F NMR (376 MHz, $CDCl_3$) δ -127.74 – -127.80 (m, 1F), -133.11 (dd, J = 20.5, 13.0 Hz, 1F), -147.10 (dd, J = 20.6, 9.5 Hz, 1F). MS (EI): calcd for $C_{11}H_6F_3N_3$ 237.1, found 237.1.

SBF3: A mixture of 2,3,5,6-tetrafluoroterephthalonitrile (0.50 g, 2.50 mmol), dimethylamine (1.13 g, 25.0 mmol), and CH_3CN (6 mL) was stirred for 5 h at 80 °C. The CH_3CN was then removed under reduced pressure. The precipitated product was filtered with water (200 mL). The residue was purified by recrystallization in acetonitrile to afford **SBF3** as orange solid (0.57 g, 92%). ^{1}H NMR (400 MHz, $CDCl_3$) δ 2.93 (s, 12H); ^{13}C NMR (100 MHz, $CDCl_3$) δ 154.7 (dd, J = 258.4, 4.0 Hz), 137.3 (dd, J = 10.0, 5.5 Hz), 111.7 (t, J = 3.2 Hz), 103.0 (dd, J = 14.2, 10.9 Hz), 43.5 (t, J = 2.2 Hz); ^{19}F NMR (376 MHz, $CDCl_3$) δ -117.25 (s, 2F). MS (EI): calcd for $C_{12}H_{12}F_2N_4$ 250.1, found 250.1.

SBF4: The compound was prepared in a similar manner as described for **SBF3.** Yield: 81% (yellow solid). ^{1}H NMR (400 MHz, $CDCl_3$) δ 4.30 (t, *J* = 7.3 Hz, 8H), 2.34 – 2.22 (m, 4H); ^{13}C NMR (100 MHz, $CDCl_3$) δ 141.7, 115.5, 109.2, 97.2, 56.2, 17.9; ^{19}F NMR (376 MHz, $CDCl_3$) δ -141.05 (s, 2F). MS (EI): calcd for $C_{14}H_{12}F_2N_4$ 274.1, found 274.1.

SBF5: The compound was prepared in a similar manner as described for **SBF3.** Yield: 94% (orange red solid). ^{1}H NMR (400 MHz, $CDCl_3$) δ 3.50 (8H), 1.88 (8H); ^{13}C NMR (100 MHz, $CDCl_3$) δ 152.5 (dd, *J* = 254.9, 3.9 Hz), 131.3 (dd, *J* = 9.9, 5.4 Hz), 113.0 (t, *J* = 3.4 Hz), 98.5 (dd, *J* = 16.5, 11.8 Hz), 51.7 (t, *J* = 2.9 Hz), 25.8; ^{19}F NMR (376 MHz, $CDCl_3$) δ -118.52 (s, 2F). MS (EI): calcd for $C_{16}H_{16}F_2N_4$ 302.1, found 302.1.

SBF6: The compound was prepared in a similar manner as described for **SBF3.** Yield: 95% (yellow solid). ^{1}H NMR (400 MHz, $CDCl_3$) δ 3.15 (8H), 1.64 (d, *J* = 4.2 Hz, 8H), 1.54 (d, *J* = 4.2 Hz, 4H); ^{13}C NMR (100 MHz, $CDCl_3$) δ 154.9 (dd, *J* = 258.7, 3.9 Hz), 137.8 (dd, *J* = 10.3, 5.7 Hz), 111.7, 104.1 (dd, *J* = 14.0, 10.9 Hz); ^{19}F NMR (376 MHz, $CDCl_3$) δ -117.57 (s, 2F). MS (EI): calcd for $C_{18}H_{20}F_2N_4$ 330.2, found 330.2.

SBF7: A mixture of **SBF3** (0.10 g, 0.40 mmol), sodium thiomethoxide (20% in water, 0.5 mL), and CH_3CN (6 mL) was stirred for 2 h at 80 °C. The CH_3CN was then removed under reduced pressure. The precipitated product was filtered with water (200 mL). Yield: 99% (orange solid). ^{1}H NMR (400 MHz, $CDCl_3$) δ 3.04 (s, 1H), 2.55 (s, 1H); ^{13}C NMR (100 MHz, $CDCl_3$) δ 154.5, 141.0, 121.1, 115.7, 43.0, 19.1; MS (EI): calcd for $C_{14}H_{18}N_4S_S$ 306.1, found 306.1.

SBF8: A mixture of 2,3,5,6-tetrafluoroterephthalonitrile (0.40 g, 2.00 mmol), malononitrile (0.27 g, 5.0 mmol), Sodium hydride (60%, 0.14 g, 6.0 mmol) and CH_3CN (6 mL) was stirred for 12 h at room temperature. Then, the solvent was removed in a rotary evaporator and the solid obtained was purified by silica gel chromatography to get light dark red powder **SBF8** (0.19 g, 30%). ^{1}H NMR (400 MHz, CD_3OD) δ 4.48 (s, 1H); ^{19}F NMR (376 MHz, CD_3OD) δ -113.28 (s, 1F), δ -119.68 (s, 1F). MS (ESI): calcd for $C_{14}HF_2N_6Na$ 314.0, found [M – Na^+] 291.1.

Mito-SBF: ^{1}H NMR (400 MHz, $CDCl_3$) δ 7.90 – 7.74 (m, 10H), 7.69 – 7.68 (m, 5H), 7.41 (s, 1H), 3.98 (2H), 3.85 (2H), 2.08 (2H); ^{13}C NMR (100 MHz, $CDCl_3$) δ 148.9, 146.4, 137.9, 137.5, 135.3 (d, J = 2.7 Hz), 133.5 (d, J = 10.0 Hz), 130.6 (d, J = 12.6 Hz), 118.2, 117.3, 111.9, 107.6, 97.1, 88.3 (dd, J = 17.8, 6.8 Hz), 43.5 (d, J = 18.6 Hz), 23.7, 20.5 (d, J = 53.0 Hz); ^{19}F NMR (376 MHz, $CDCl_3$) δ -120.95 (dd, *J* = 12.4, 7.1 Hz, 1F), -133.65 (dd, *J* = 20.2, 12.4 Hz, 1F), -148.43 (dd, *J* = 20.5, 7.1 Hz, 1F). MS (ESI): calcd for $C_{29}H_{22}F_3N_3P^+$ 500.2, found 500.2.

BSA-SBF: ^{1}H NMR (400 MHz, $CDCl_3$) δ 6.28 (dd, *J* = 16.9, 1.2 Hz, 1H), 6.06 (dd, *J* = 16.9, 10.3 Hz, 1H), 5.66 (dd, *J* = 10.3, 1.1 Hz, 1H), 5.48 (1H), 4.39 (1H), 3.92 (2H), 2.19 – 2.13 (m, 4H), 1.46 – 1.30 (m, 4H); ^{13}C NMR (100 MHz, $CDCl_3$) δ 165.4, 149.2, 146.1, 139.2 (dddd, J = 67.3, 18.4, 15.2, 4.3 Hz), 136.1 (dd, J = 33.7, 12.2 Hz), 130.8 (d, J = 4.0 Hz), 126.5 (d, J = 12.2 Hz), 111.1 (d, J = 28.4 Hz), 107.6 (d, J = 3.6 Hz), 97.7 (dd, J = 38.6, 19.3 Hz), 90.6 (dd, J = 17.7, 7.0 Hz), 52.6, 47.4, 32.5, 30.8, 28.9, 27.5; ^{19}F NMR (376 MHz, $CDCl_3$) δ -126.43 (dd, *J* = 13.1, 7.8 Hz, 1F), -131.80 (dd, *J* = 20.2, 13.1 Hz, 1F), -145.13 (dd, *J* = 20.5, 7.8 Hz, 1F). MS (ESI): calcd for $C_{17}H_{15}F_3N_4O$ 348.1, found 348.2.

HClO-SBF: ^{1}H NMR (400 MHz, $CDCl_3$) δ 3.58 (4H), 2.83 (4H); ^{13}C NMR (100 MHz, $CDCl_3$) δ 154.9, 152.3, 149.3 (dd, *J* = 13.3, 4.0 Hz), 146.6 (ddd, *J* = 16.0, 11.5, 4.6 Hz), 143.9 (d, *J* = 14.9 Hz), 140.4 (dd, *J* = 12.5, 3.5 Hz), 110.3 (t, *J* = 3.9 Hz), 107.2 (d, *J* = 3.7 Hz), 53.9, 28.0; ^{19}F NMR (376 MHz, $CDCl_3$) δ -115.74 (d, *J* = 13.0 Hz, 1F), -129.83 (dd, *J* = 19.7, 14.3 Hz, 1F), -133.12 (d, *J* = 20.7 Hz, 1F). MS (EI): calcd for $C_{12}H_8F_3N_3S$ 283.0, found 283.1.

4 Optical spectra, calculations and biological studies

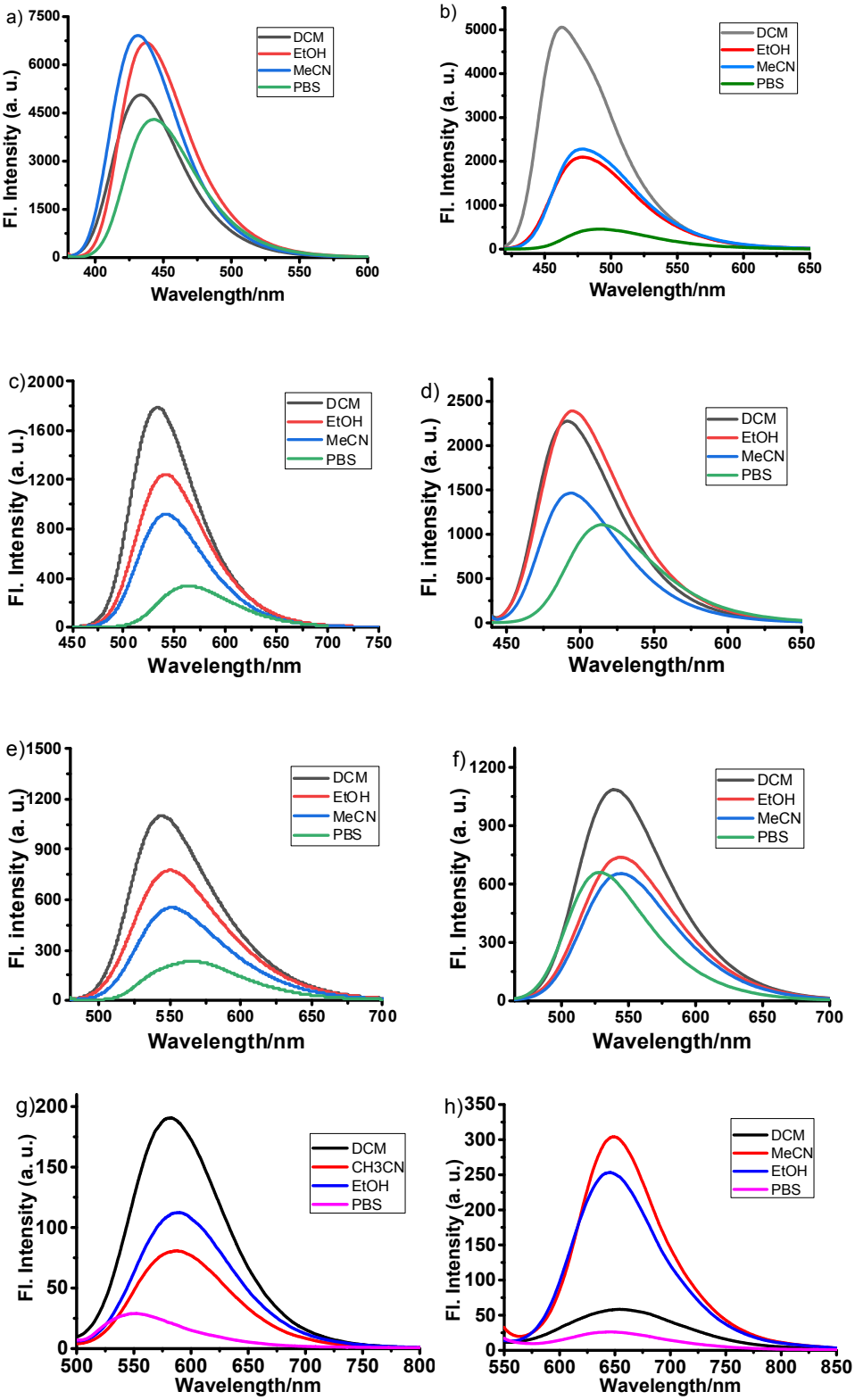

Fig. S1. Fluorescence emission spectra of (a) **SBF1**, (b) **SBF2**, (c) **SBF3**, (d) **SBF4**, (e) **SBF5,** (f) **SBF6,** (g) **SBF7** and (h) **SBF8** in various solvents at 25 ^{o}C by excitation at their respective maximum absorption wavelengths.

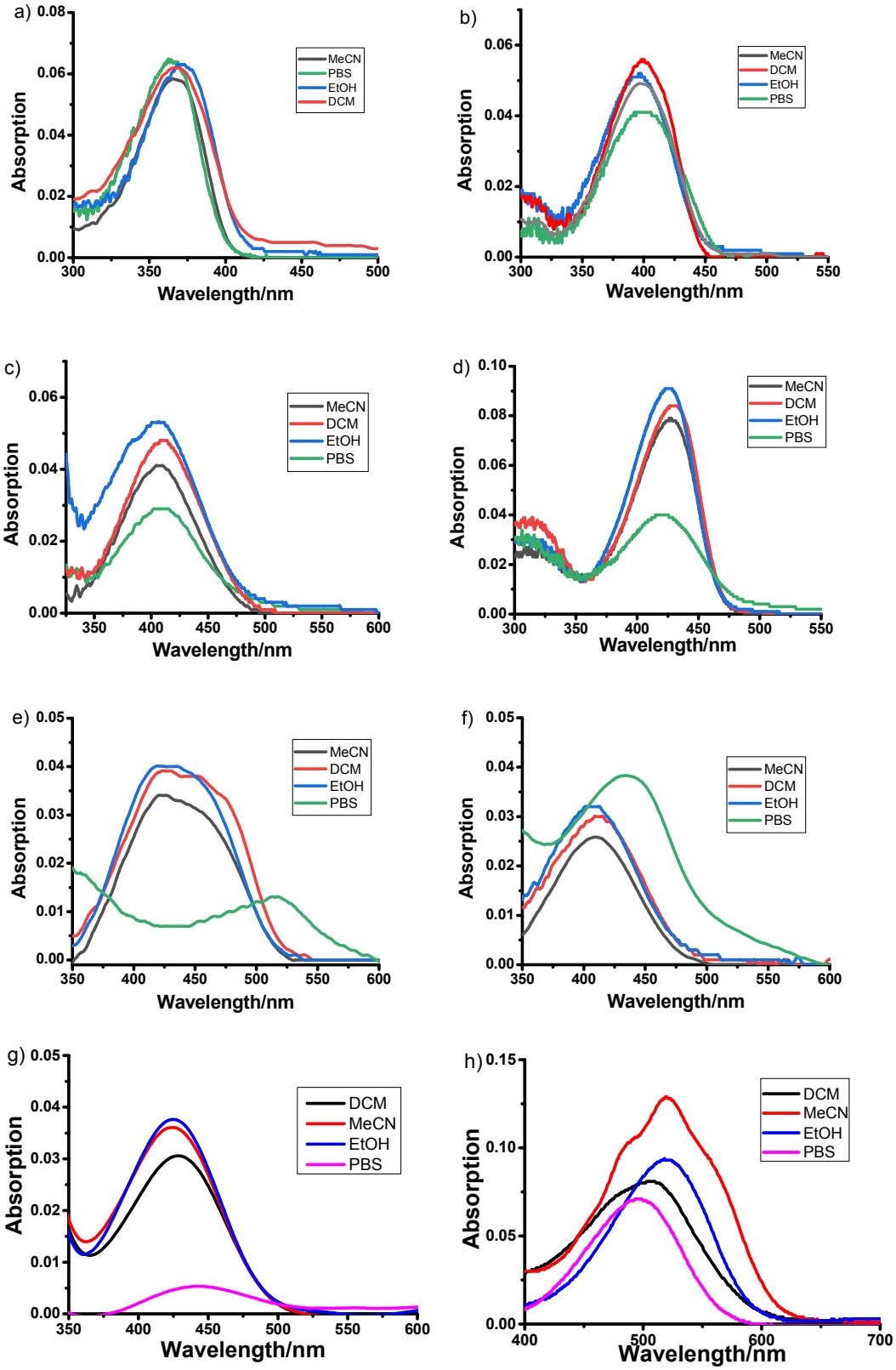

Fig. S2. Absorption spectra of **SBF1-8** (10 μM) in various solvents at 25 °C.

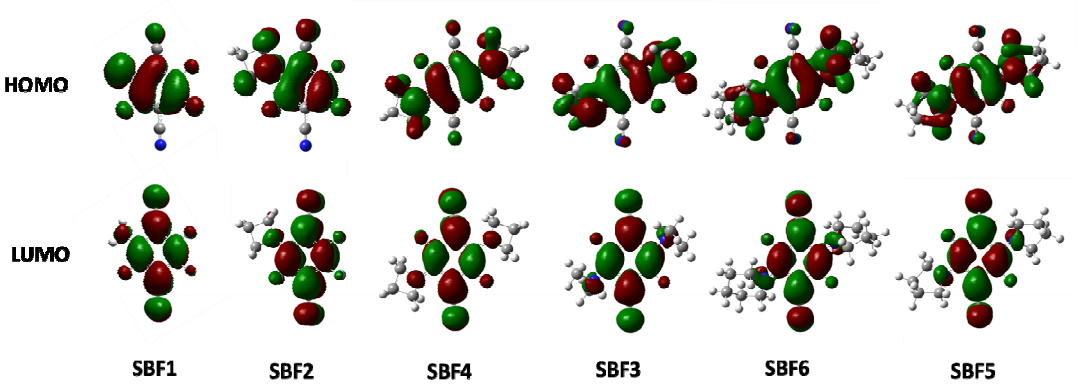

Fig. S3. DFT optimized molecular orbital plots (LUMO and HOMO) of **SBF1-SBF6**.

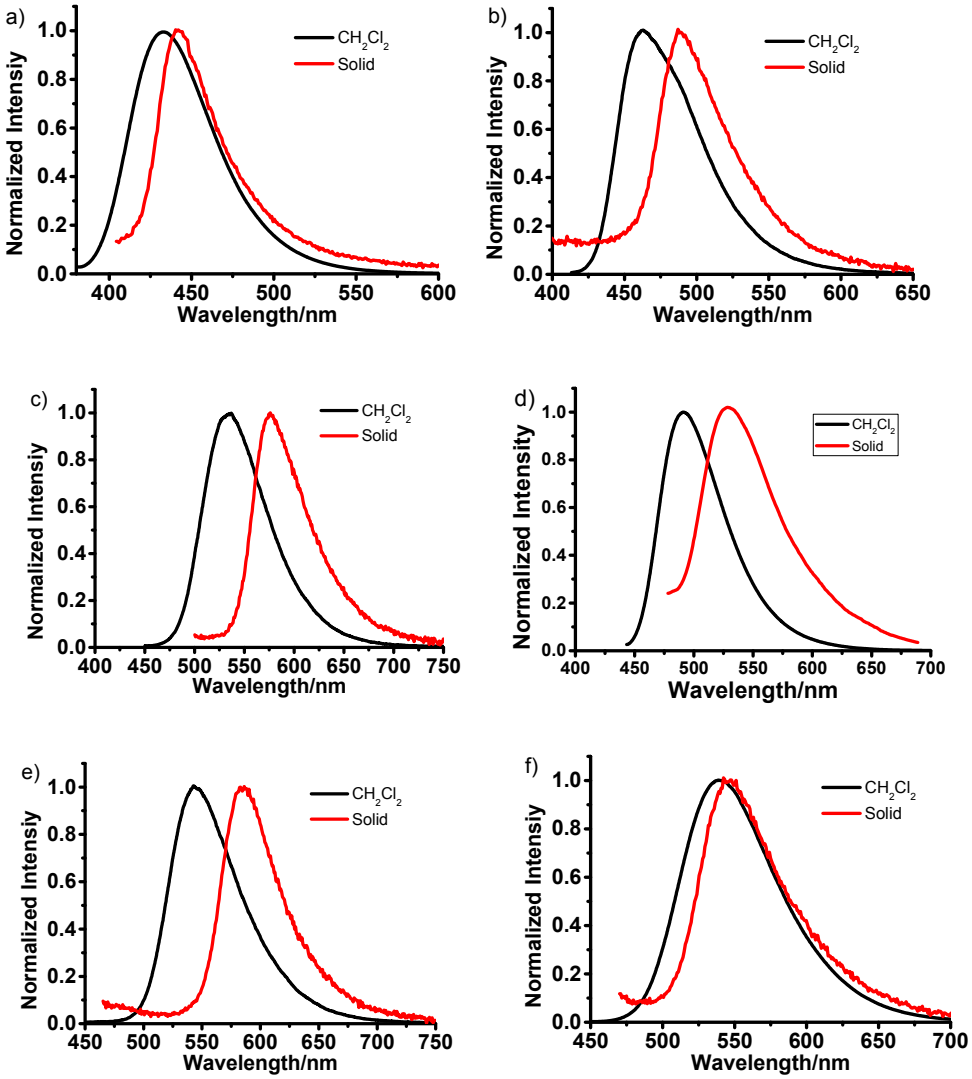

Fig. S4. (a)–(g) The normalized emission spectras of **SBF1-6** in CH_2Cl_2 solution (black line) and solid-state (red line).

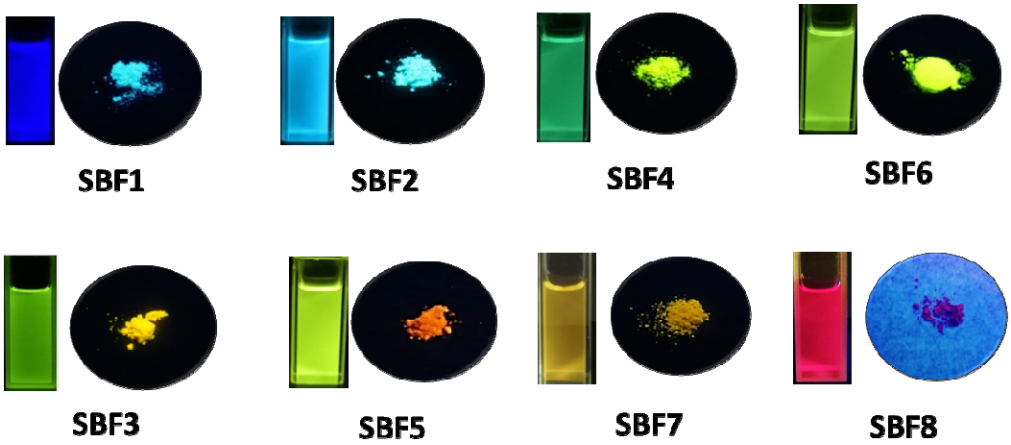

Fig. S5. Photographs of **SBF1-8** in CH_2Cl_2 solution and solid-state under UV light (365 nm).

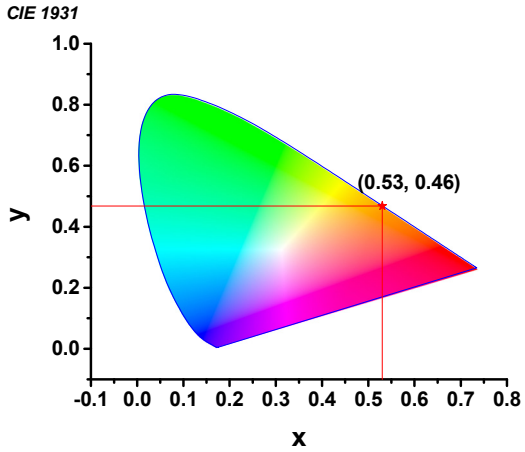

Fig. S6. CIE coordinates of the emissions of solid **SBF3**.

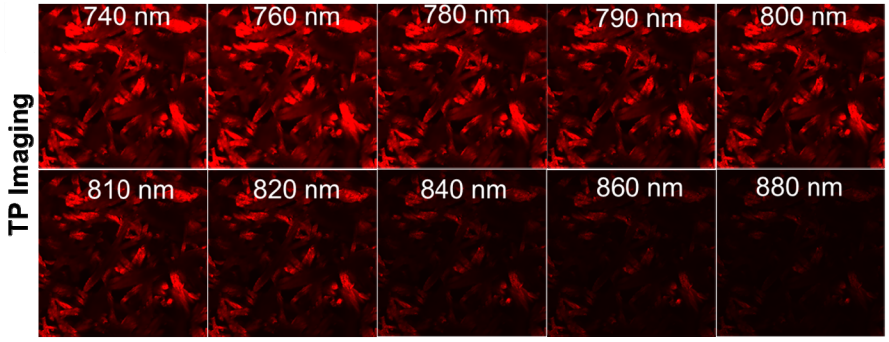

Fig. S7. Two-photon pseudo-colored fluorescence images of solid SBF3, the images were recorded at yellow channel (540–580 nm) upon excitation from 740 nm to 880 nm with femtosecond laser pulse (Olympus FV1000).

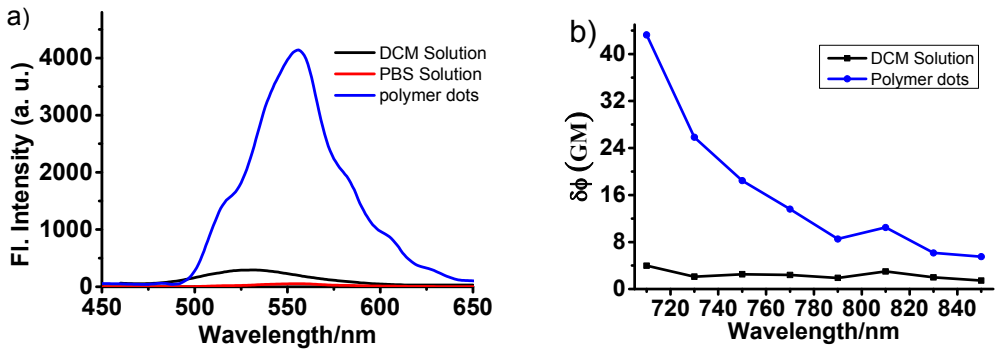

Fig. S8. a) Two-photon emission spectra (Excitation: 710 nm) and (b) two-photon action cross sections of **SBF3** in its solution and solid-state (polymer dots).

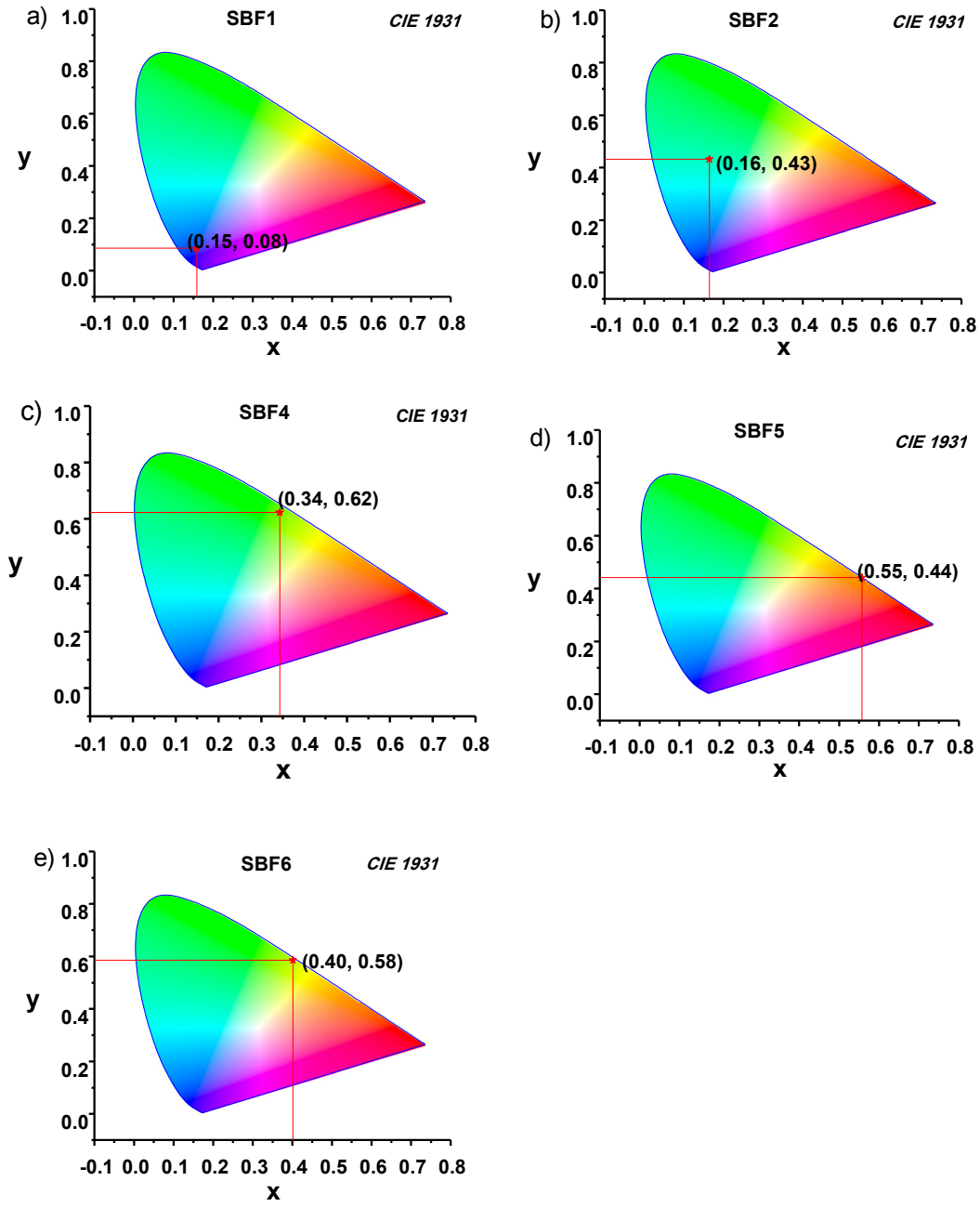

Fig. S9. CIE coordinates of the emissions of solids **SBF1-2** and **SBF4-6**.

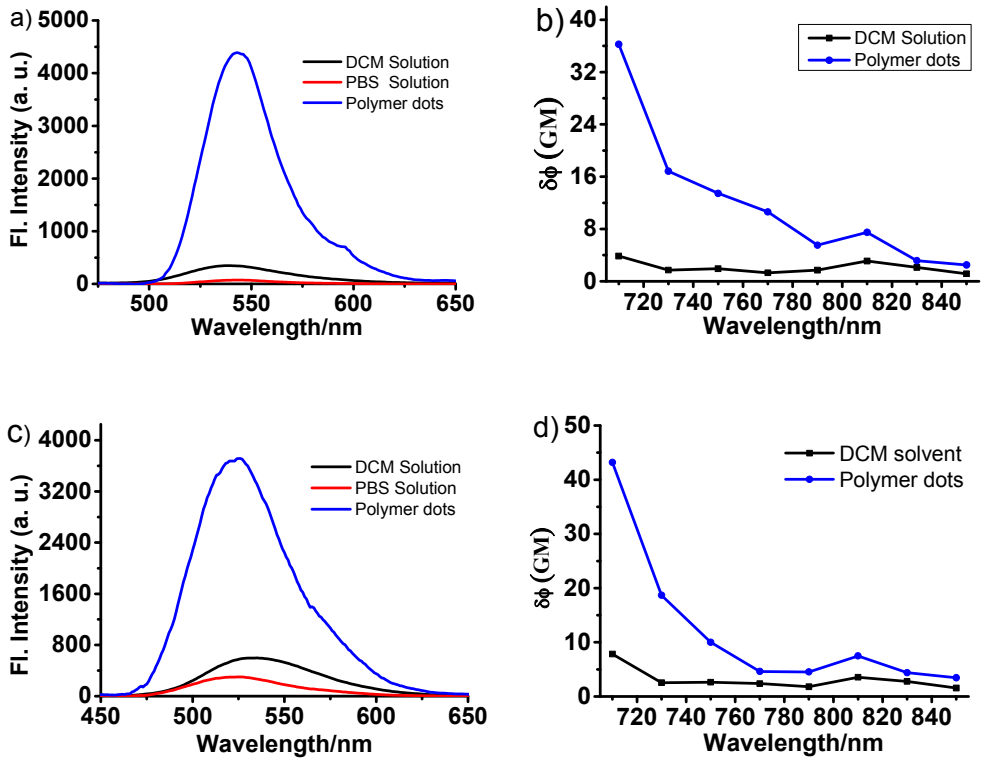

Fig. S10. a) Two-photon emission spectra (Excitation: 710 nm) and (b) two-photon action cross sections of **SBF5** in its solution and solid-state (polymer dots). c) Two-photon emission spectra (Excitation: 710 nm) and (d) two-photon action cross sections of **SBF6** in its solution and solid-state (polymer dots)**.**

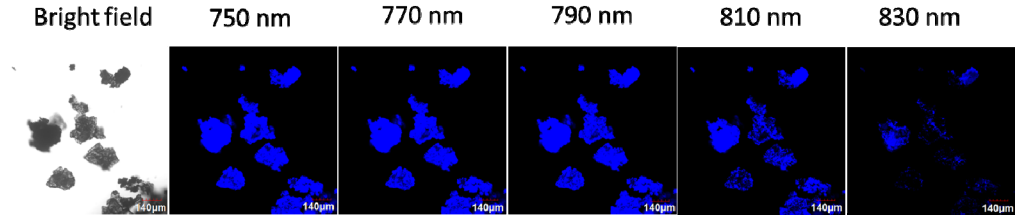

Fig. S11. Two-photon pseudo-colored fluorescence images of solid **SBF1**, the images were recorded at yellow channel (420–460 nm) upon excitation from 750 nm to 830 nm at 20 nm interval with femtosecond laser pulse (Olympus FV1000).

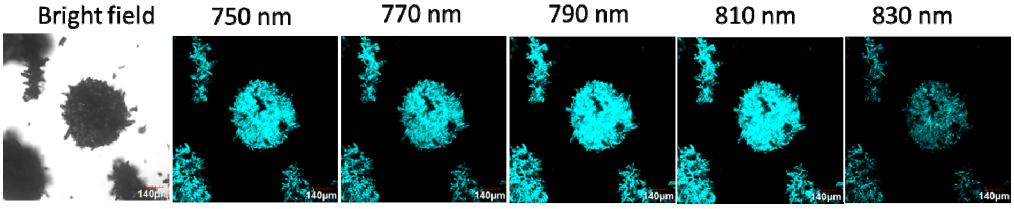

Fig. S12. Two-photon pseudo-colored fluorescence images of solid **SBF2**, the images were recorded at yellow channel (450–490 nm) upon excitation from 750 nm to 830 nm at 20 nm interval with femtosecond laser pulse (Olympus FV1000).

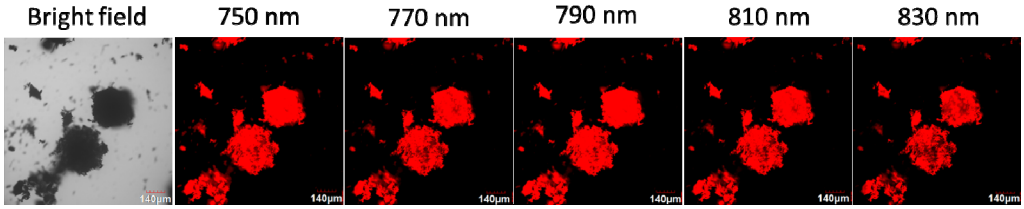

Fig. S13. Two-photon pseudo-colored fluorescence images of solid **SBF5**, the images were recorded at red channel (575–630 nm) upon excitation from 750 nm to 830 nm at 20 nm interval with femtosecond laser pulse (Olympus FV1000).

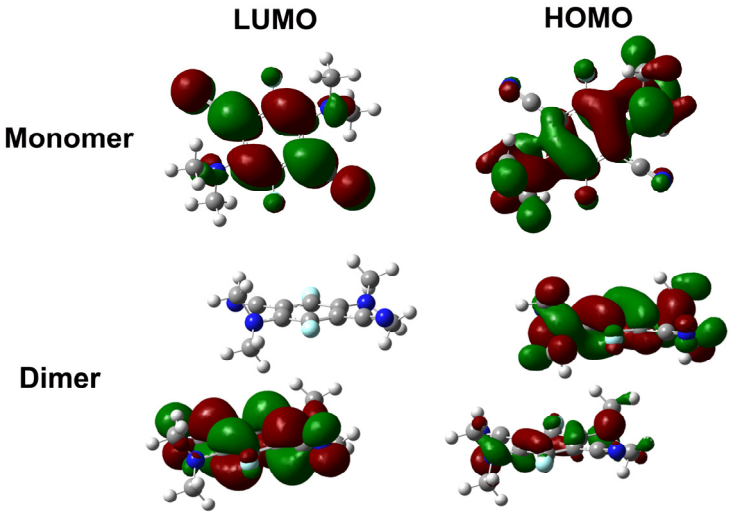

Fig. S14. DFT optimized structures and molecular orbital plots (LUMO and HOMO) of SBF3 in its monomer and dimer states. Water was used as the solvent for calculations at the B3LYP/6-31G(d) level.

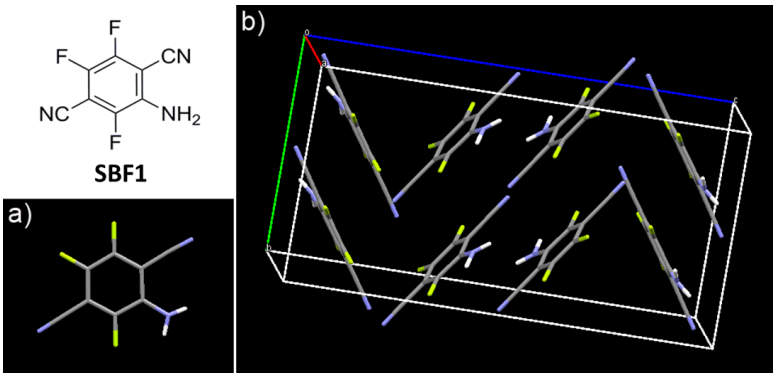

Fig. S15. a) Crystal structure of **SBF1**. b) Packing structure in a cell.

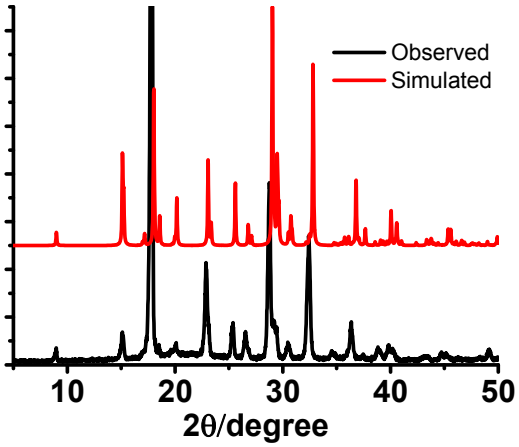

Fig. S16. Observed (black) and simulated (red) powder X-ray diffraction patterns for **SBF1**.

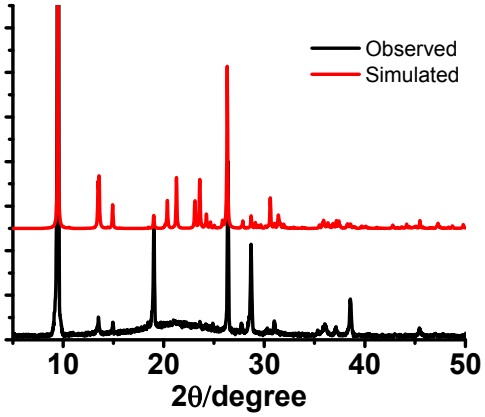

Fig. S17. Observed (black) and simulated (red) powder X-ray diffraction patterns for **SBF3**.

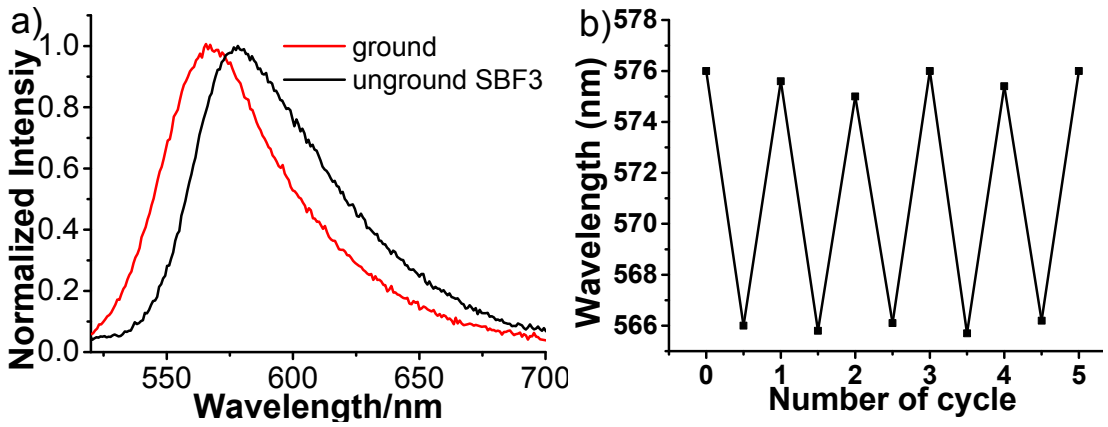

Fig. S18. a) Spectra of unground and ground SBF3; b) Reversible switching of the emission of SBF3 by repeated grinding/fuming cycles.

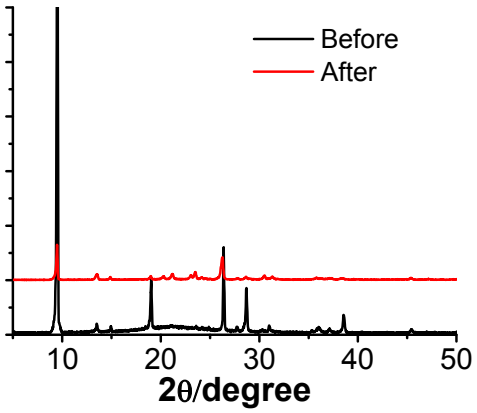

Fig. S19. Powder X-Ray diffraction of unground **SBF3** (black) and ground **SBF3** (red).

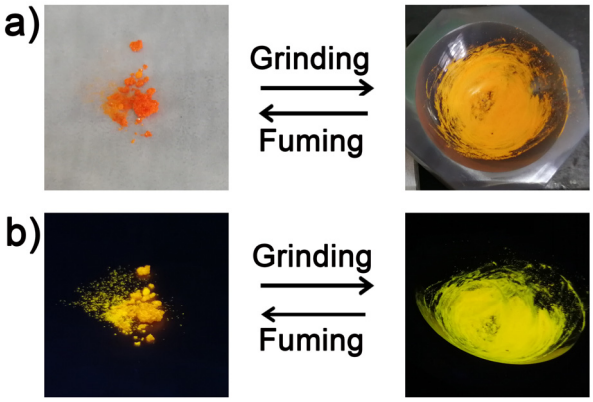

Fig. S20. Photographs of as-prepared **SBF5** and after grinding under (a) visible light and (b) 365 nm irradiation.

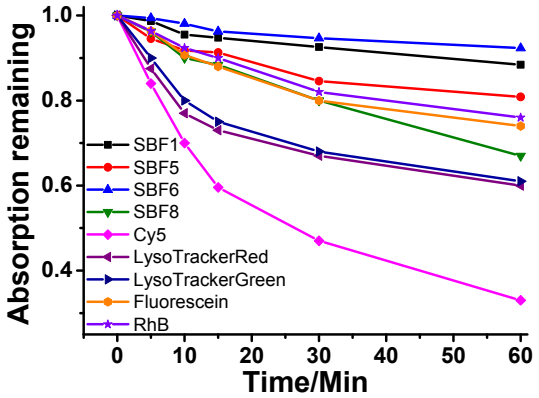

Fig. S21. Photostability of representative **SB-Fluors**, Cy5, Lyso-Tracker Green, Lyso-Tracker Red, fluorescein and Rhodamine B (RhB) in PBS buffer solution (pH 7.4). The samples were continuously irradiated by white light (50 W) in ice-bath condition.

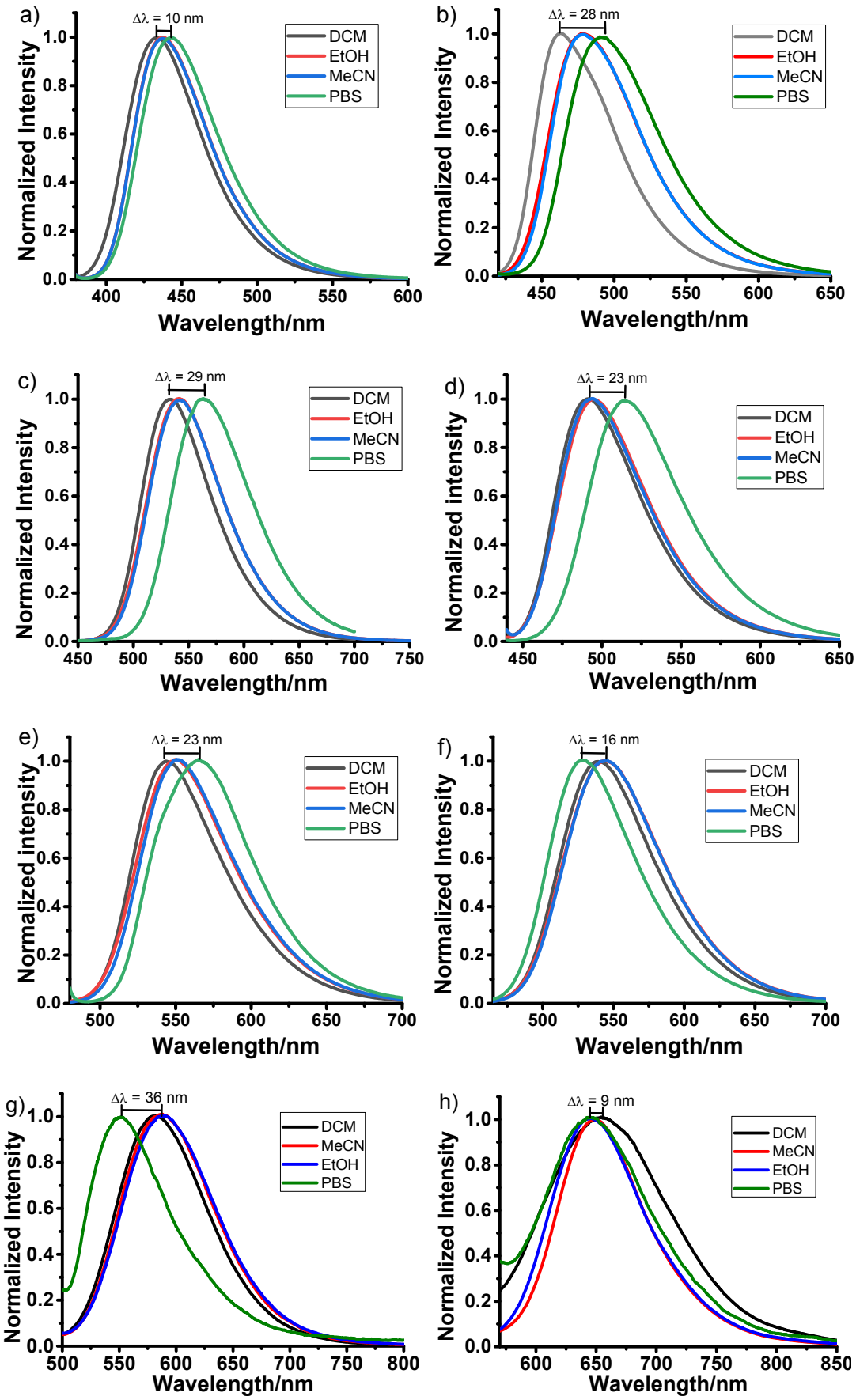

Fig. S22. Normalized emission spectra of (a) **SBF1**, (b) **SBF2**, (c) **SBF3**, (d) **SBF4**, (e) **SBF5**, (f)

SBF6, (g) **SBF7** and (h) **SBF8** in various solvents at 25 °C by excitation at their respective maximum absorption wavelengths.

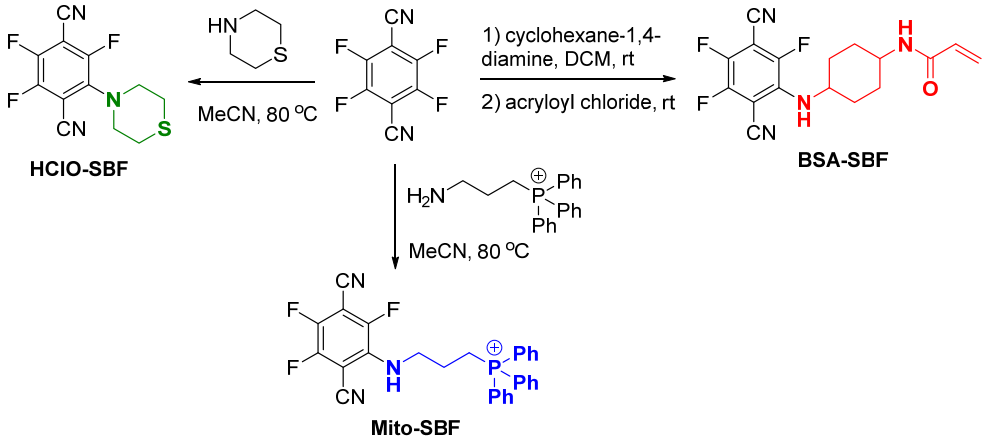

Fig. S23. Design and synthesis of probe **HClO-SBF** and biomarker reagent **BSA-SBF** /**Mito-SBF.**

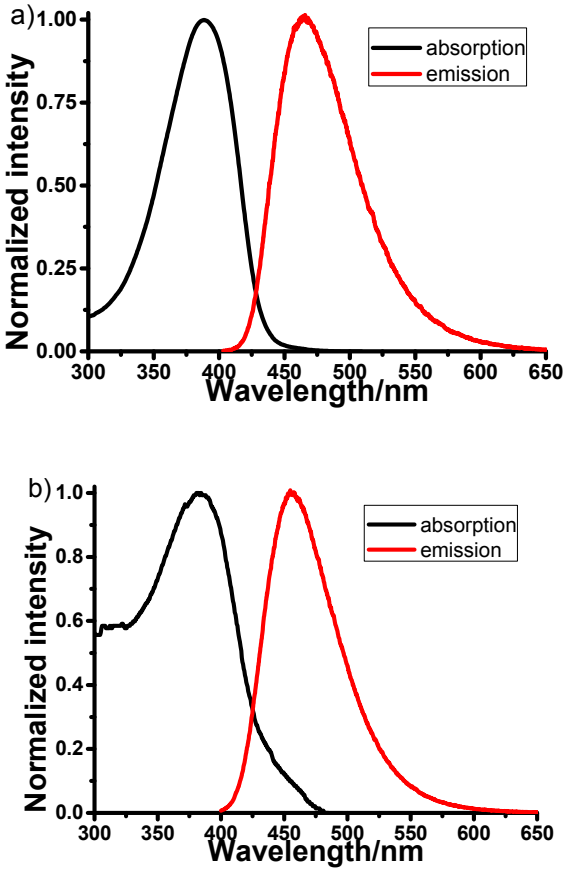

Fig. S24. Normalized absorption and emission spectras of (a) **BSA-SBF** and (b) **Mito-SBF** in PBS buffer (25 mM, pH 7.4) at 25 °C**.**

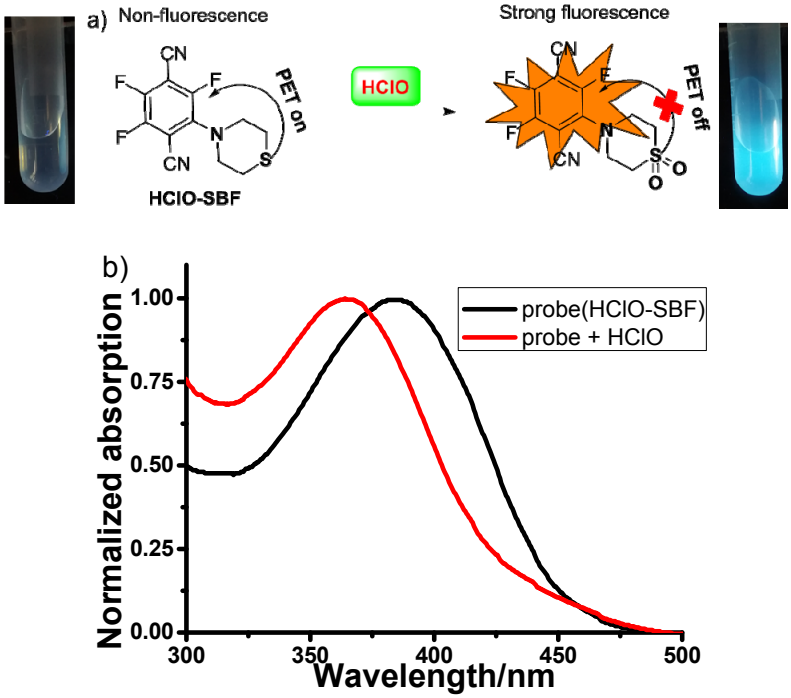

Fig. S25. (a) Possible reaction mechanism of probe for HClO. (b) Normalized absorption spectra of probe **HClO-SBF** and **HClO-SBF** added with 200 μM HClO in PBS buffer (25 mM, pH 7.4) at 25 °C

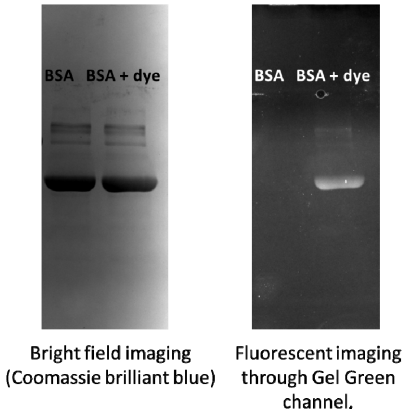

Fig. S26. SDS-PAGE analysis of purified BSA and the labeling reaction of BSA with **BSA-SBF**.

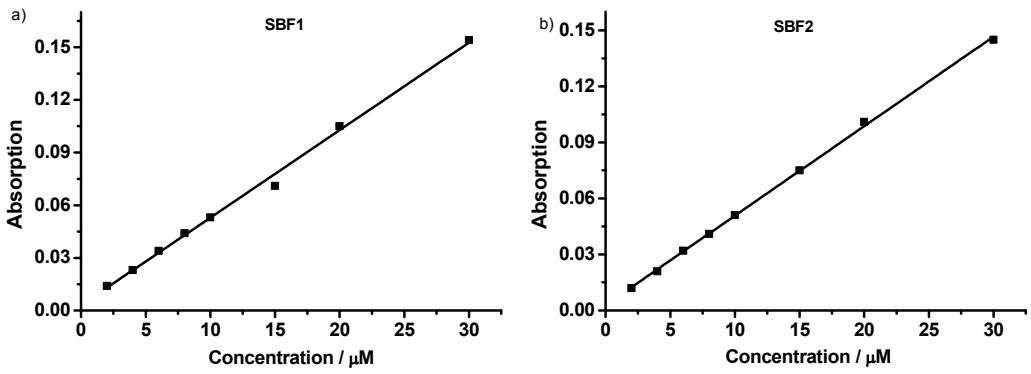

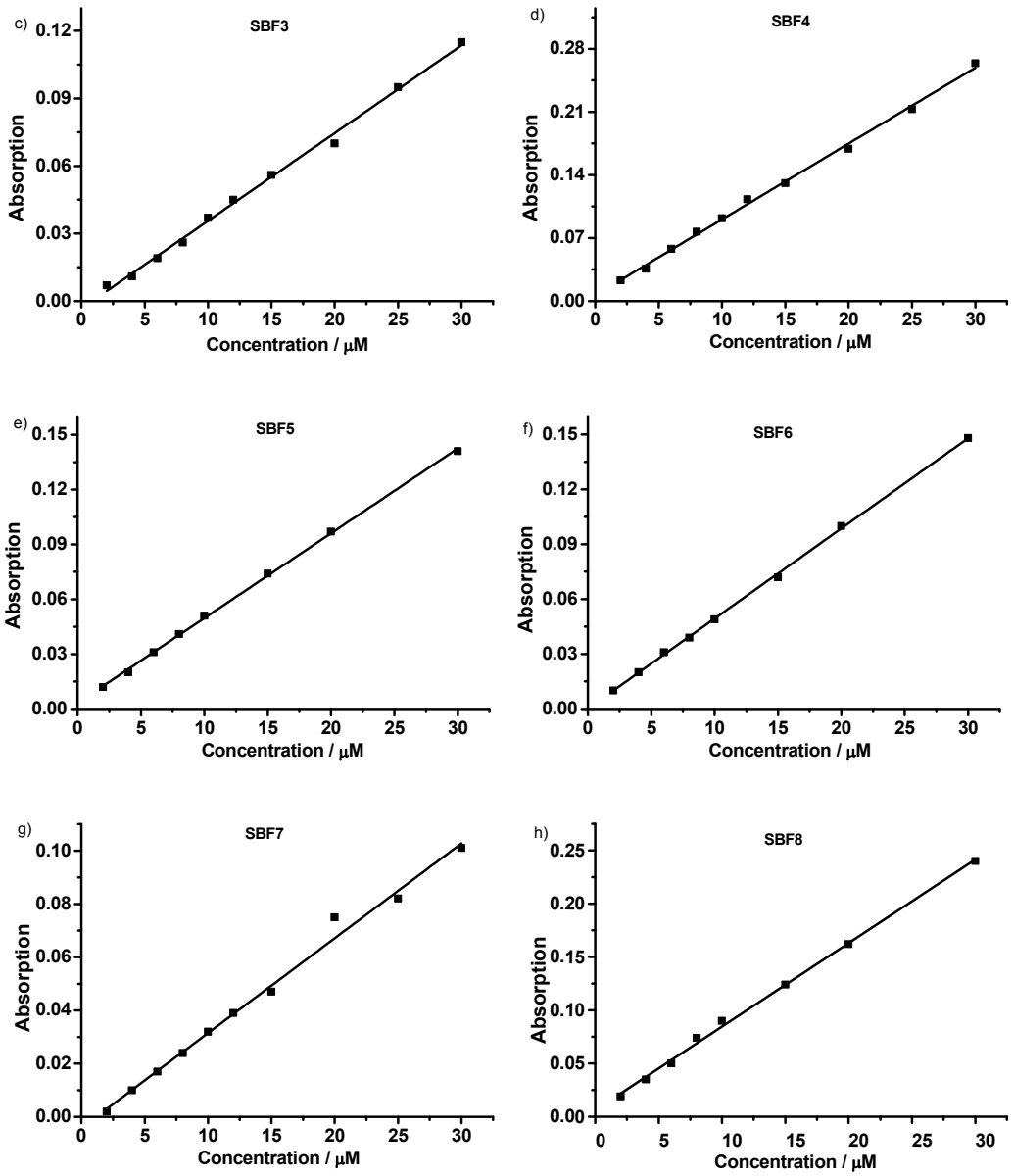

Fig. S27. (a-h) Linear correlation between the absorption and concentration of **SBF1-8** (2 – 30 μM) in MeCN.

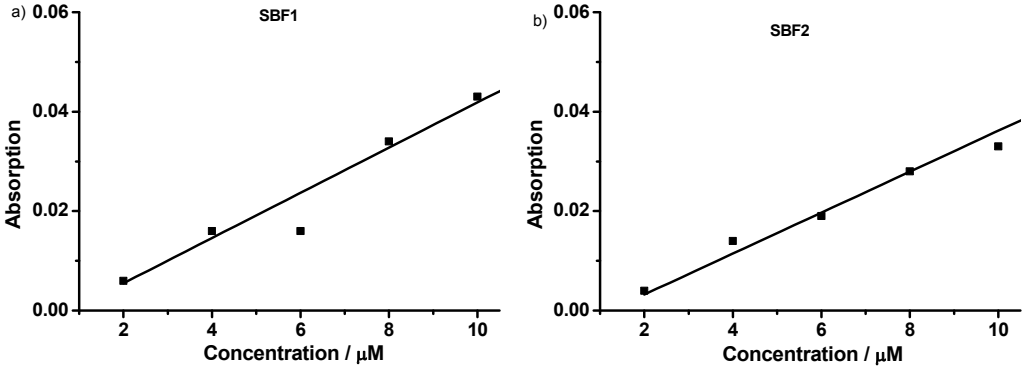

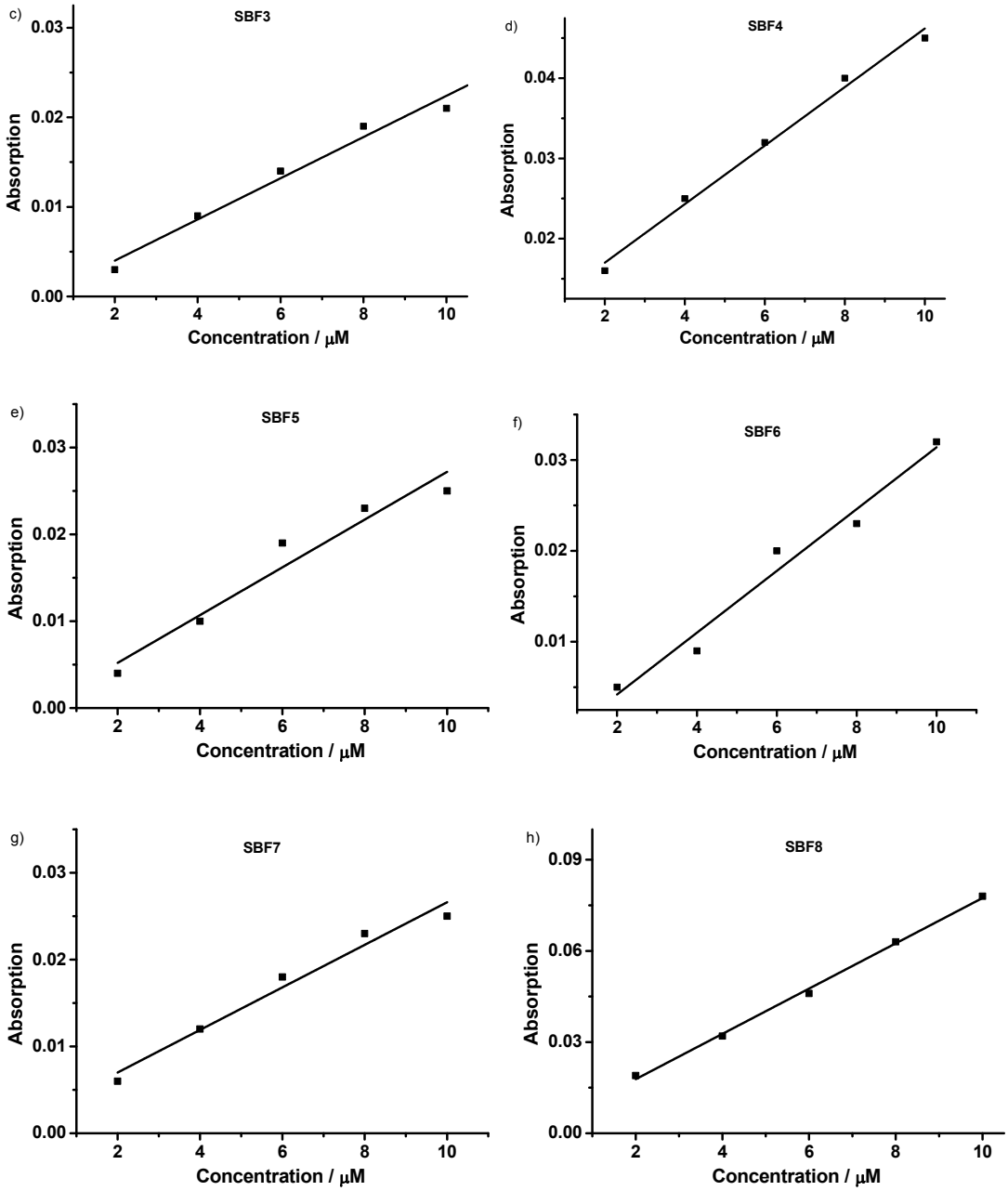

Fig. S28. (a-h) Linear correlation between the absorption and concentration of **SBF1-8** (2 – 10 μM) in PBS buffer.

NMR spectra

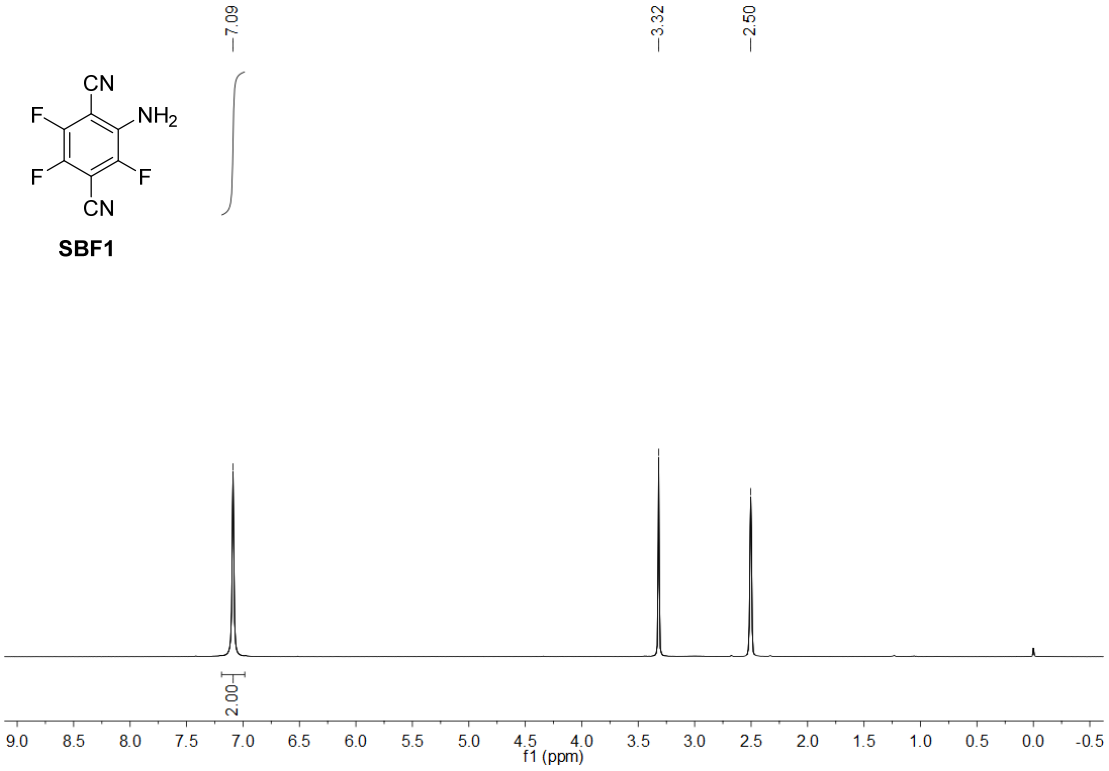

^{1}H NMR spectrum of **SBF1.**

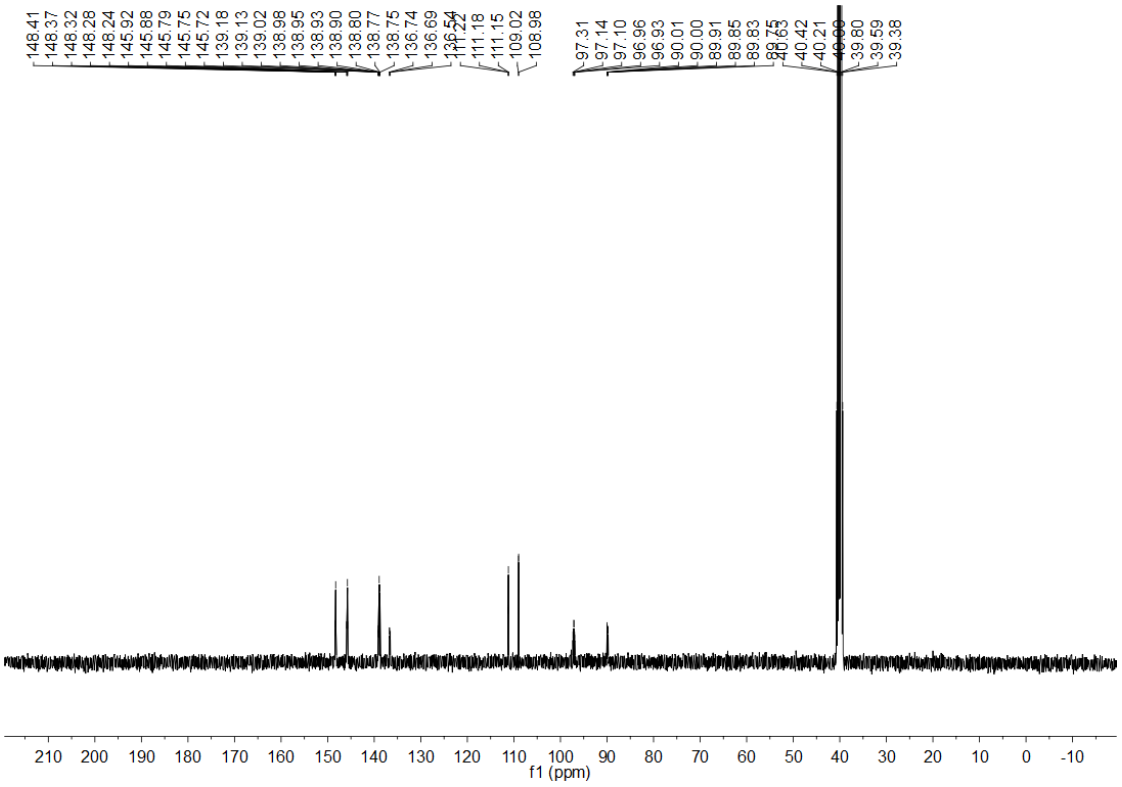

^{13}C NMR spectrum of **SBF1.**

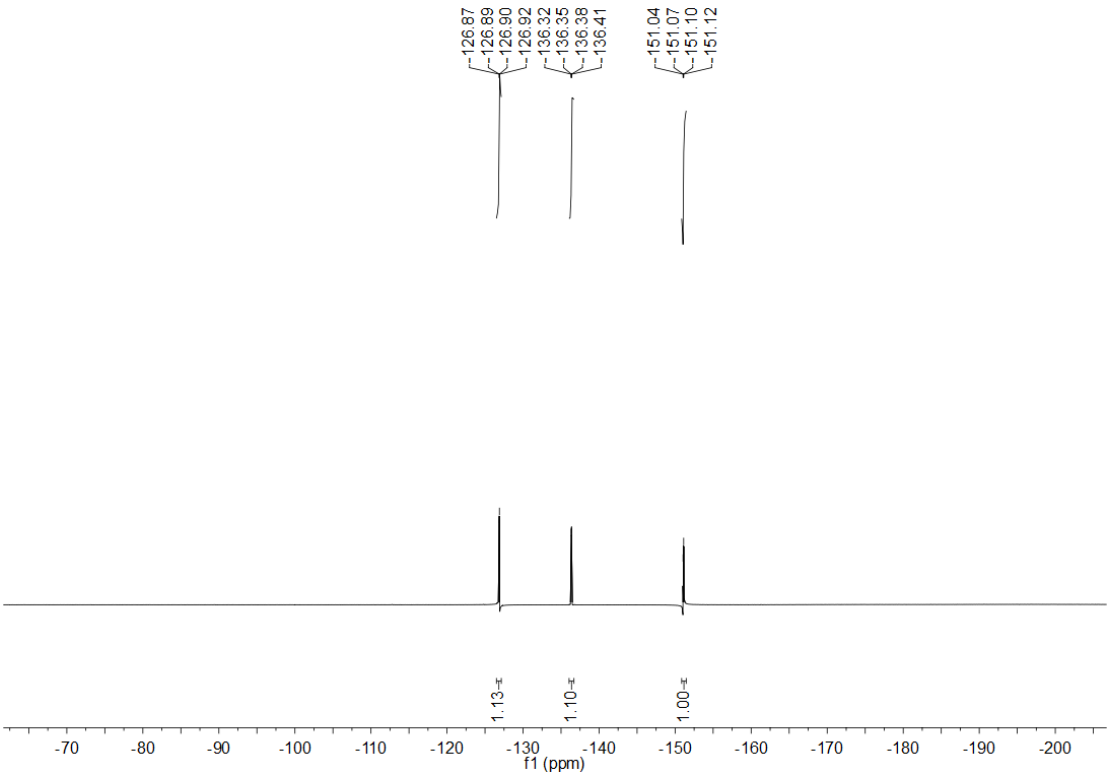

^{19}F NMR spectrum of **SBF1.**

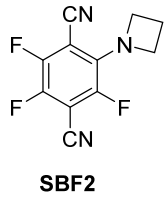

SBF2

^{1}H NMR spectrum of **SBF2.**

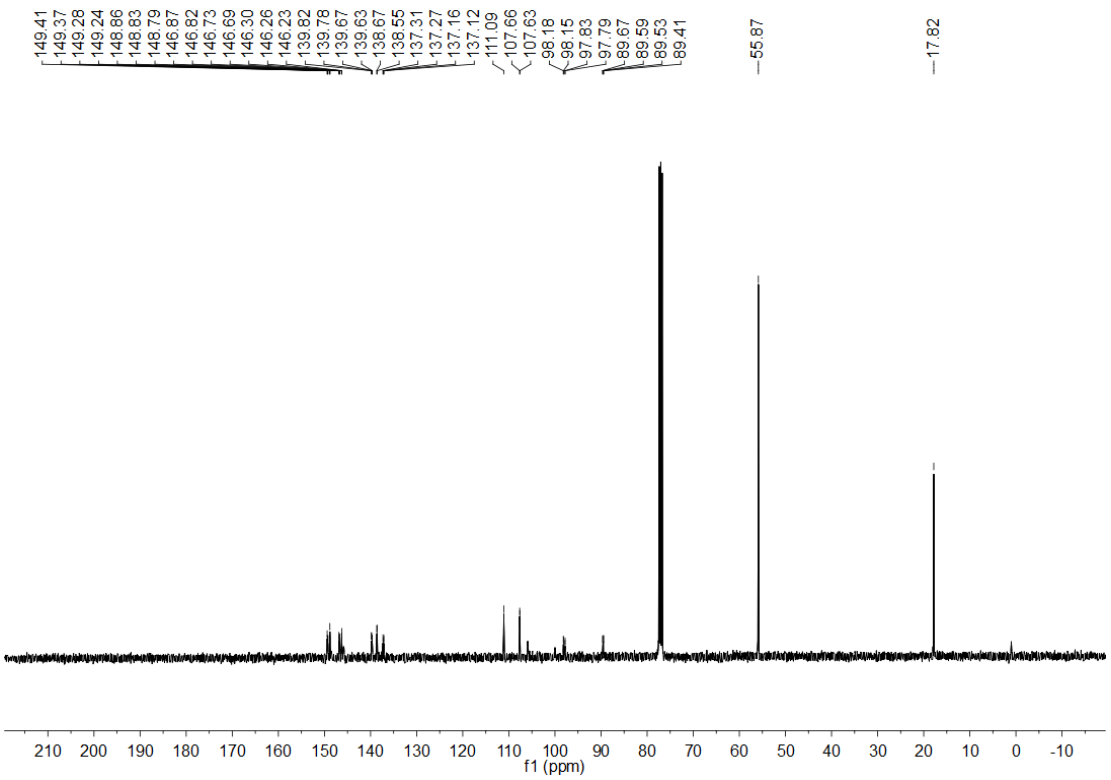

^{13}C NMR spectrum of **SBF2.**

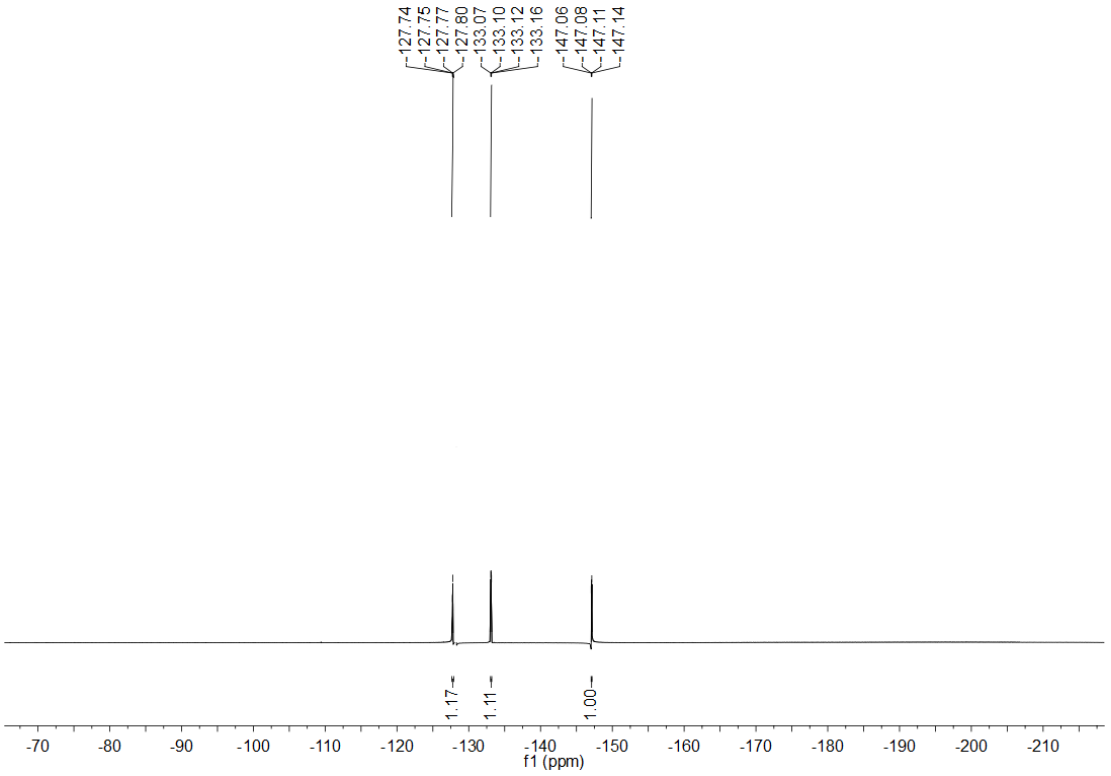

^{19}F NMR spectrum of **SBF2.**

SBF3

^{1}H NMR spectrum of **SBF3.**

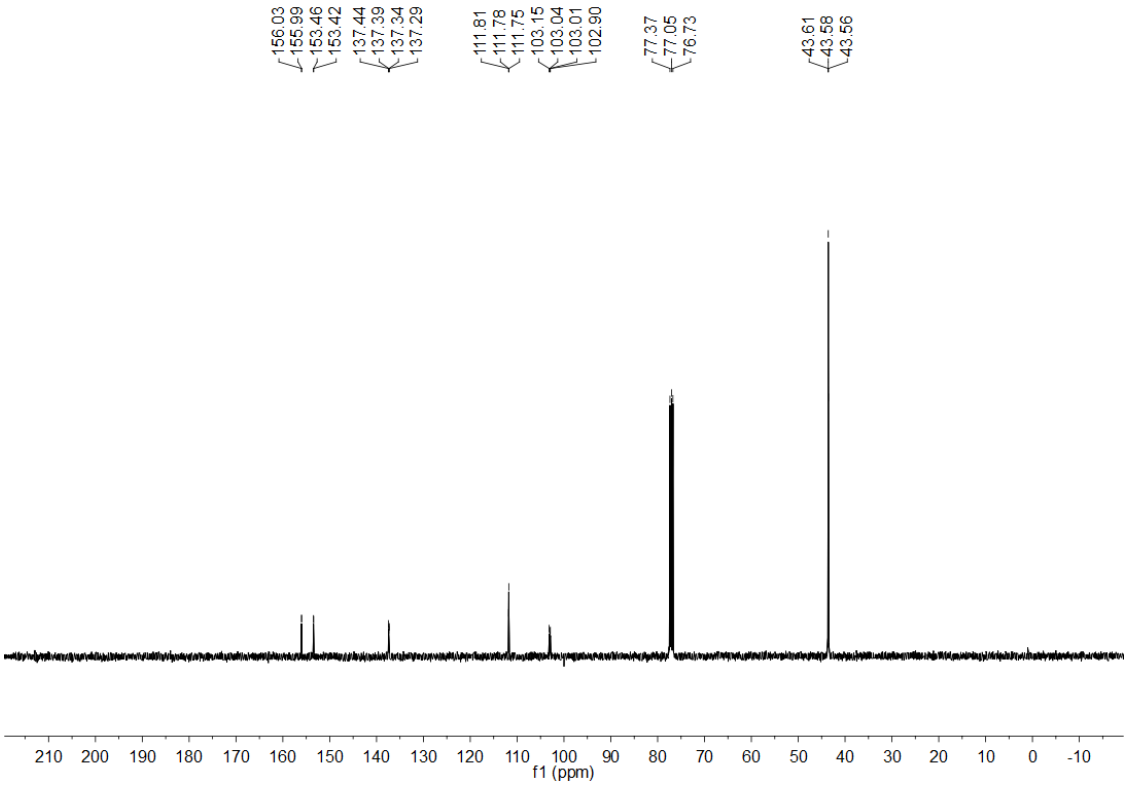

^{13}C NMR spectrum of **SBF3.**

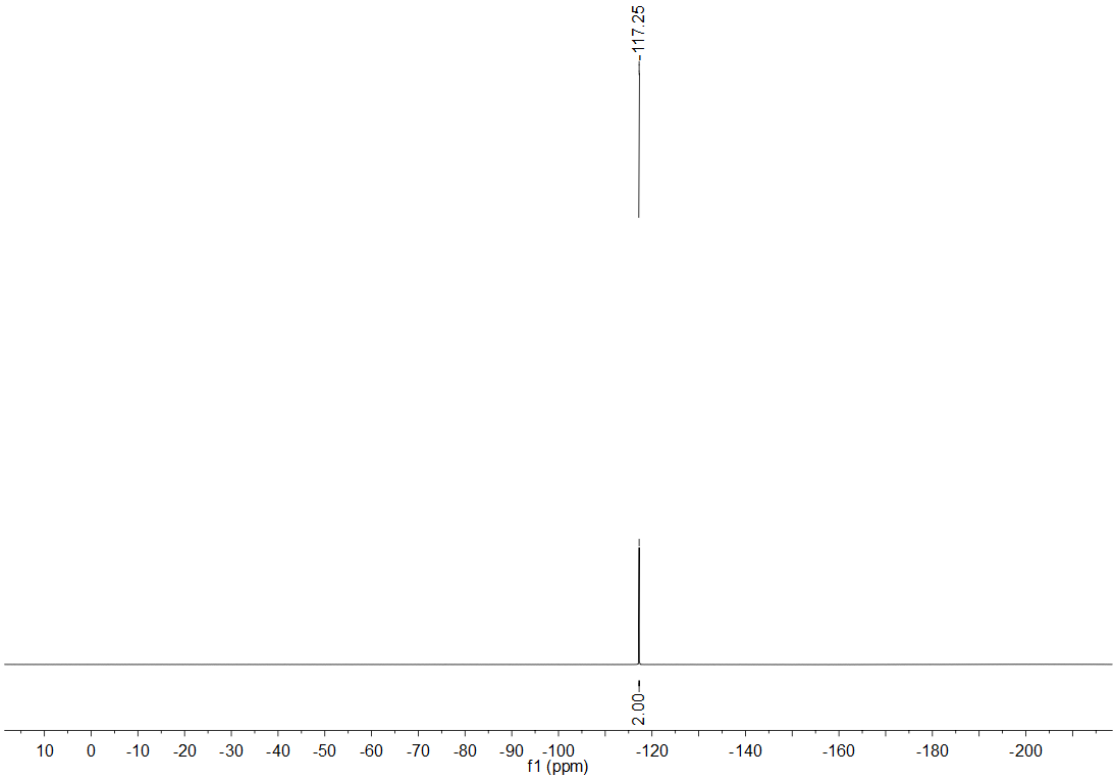

^{19}F NMR spectrum of **SBF3.**

SBF4

^{1}H NMR spectrum of **SBF4.**

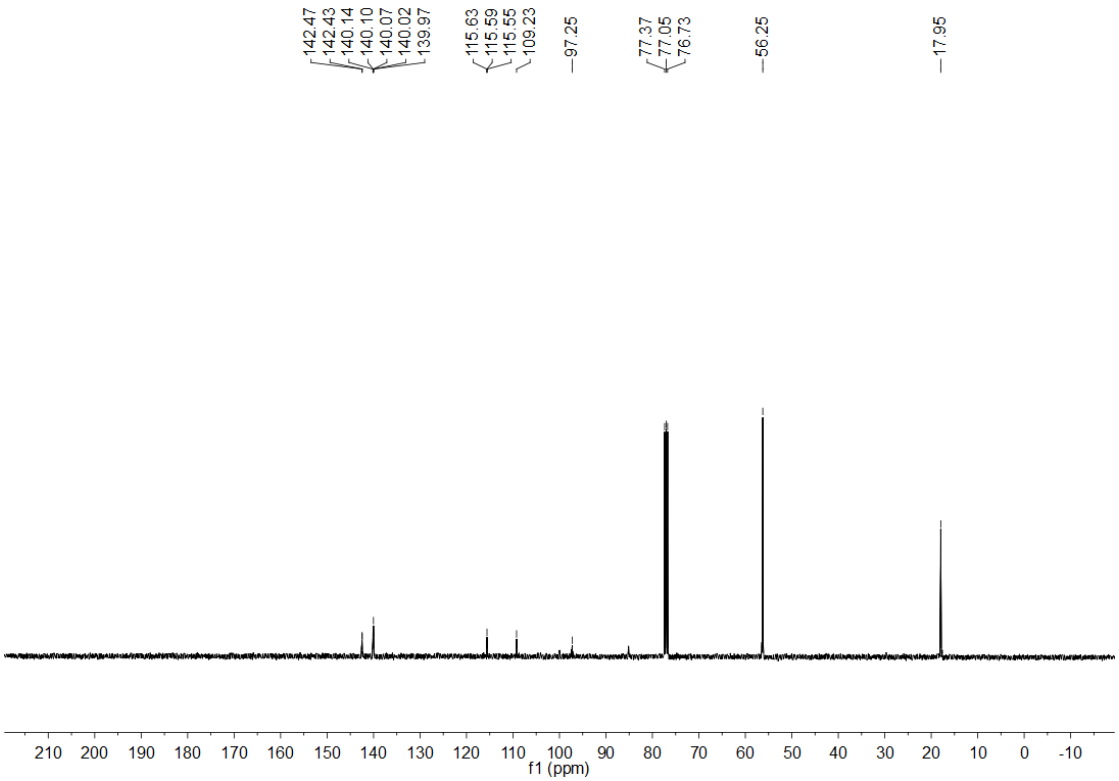

^{13}C NMR spectrum of **SBF4.**

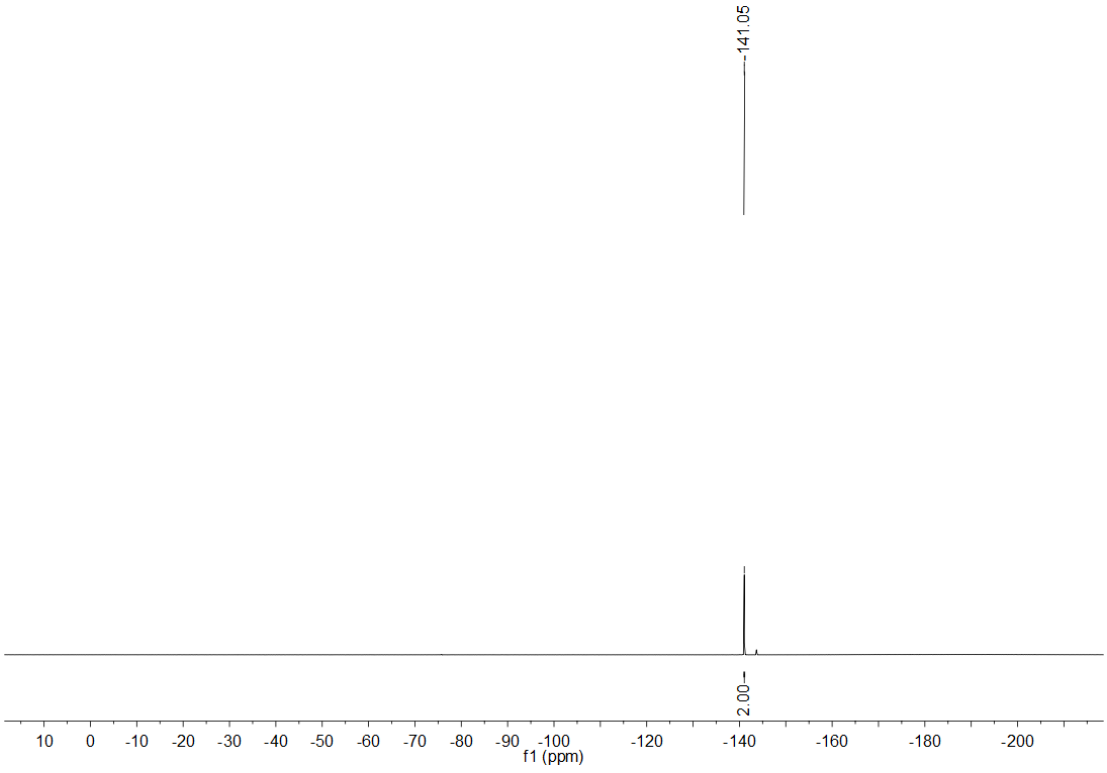

^{19}F NMR spectrum of **SBF4.**

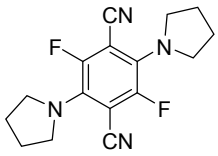

SBF5

^{1}H NMR spectrum of **SBF5.**

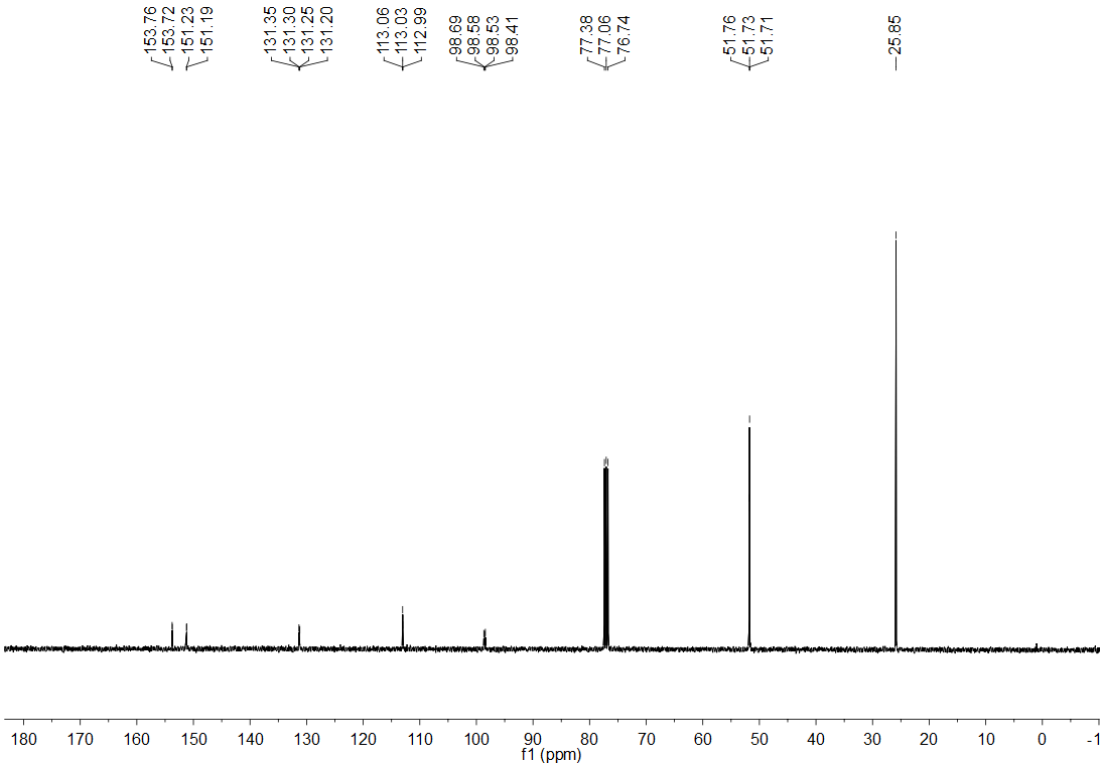

^{13}C NMR spectrum of **SBF5.**

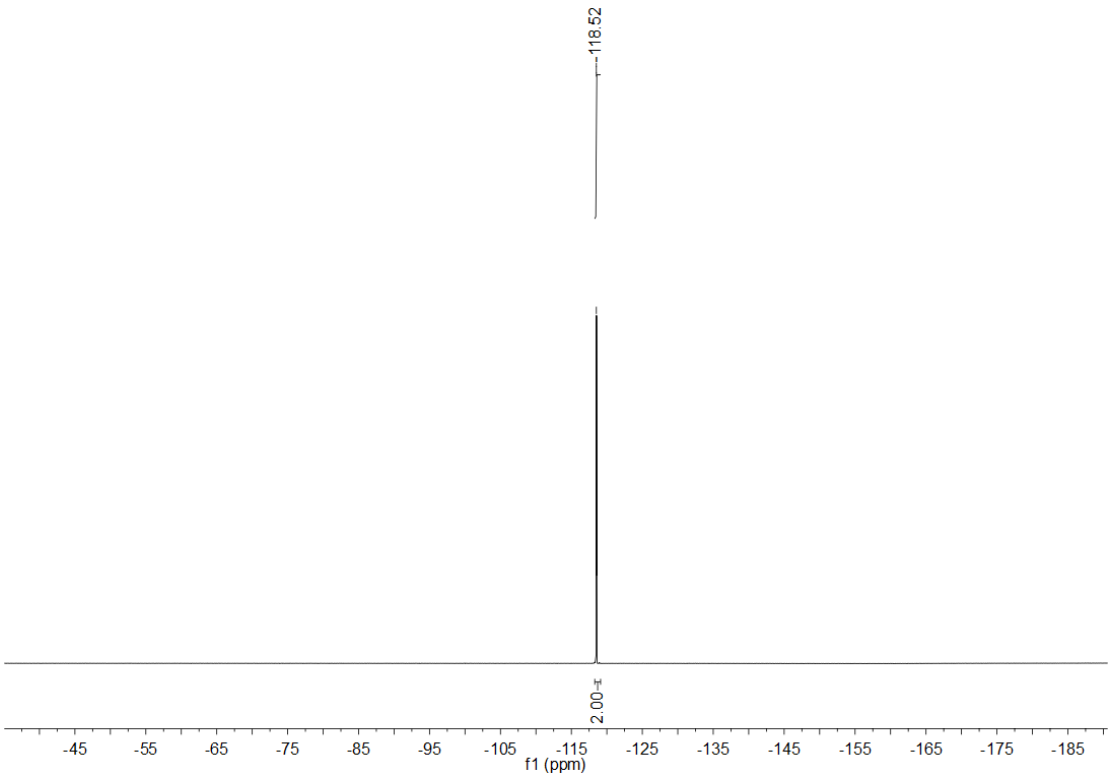

^{19}F NMR spectrum of **SBF5.**

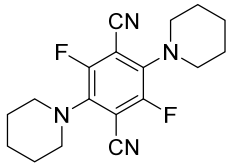

SBF6

^{1}H NMR spectrum of **SBF6.**

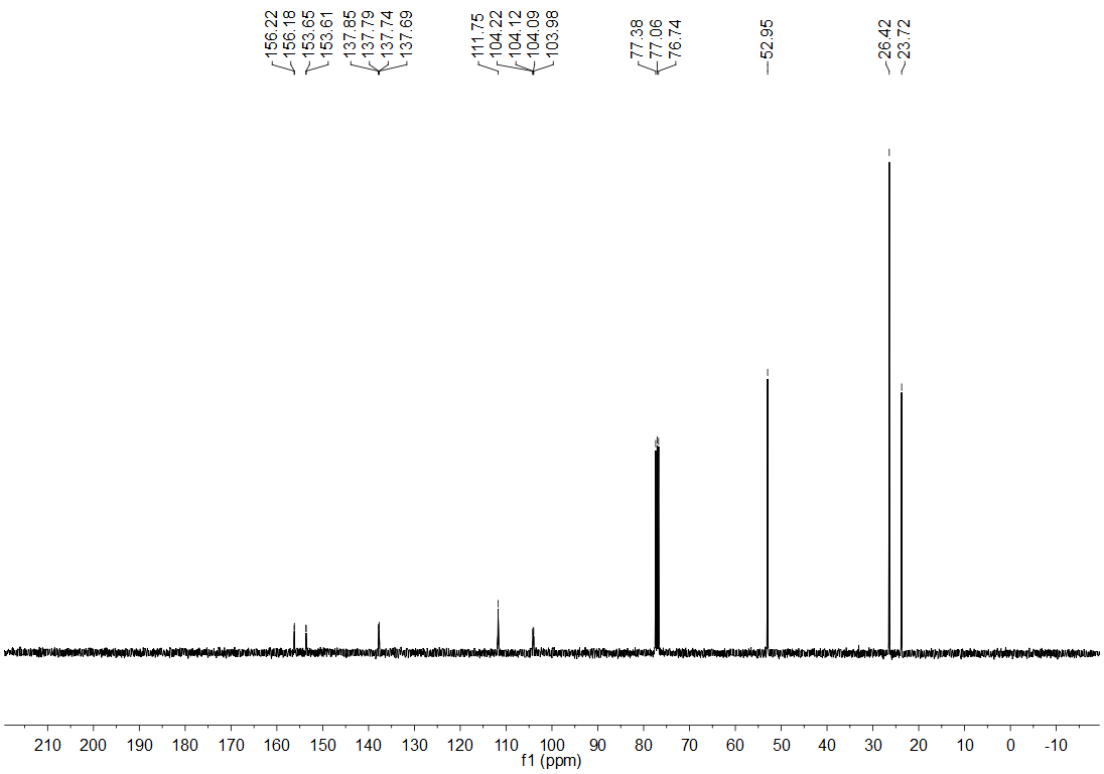

^{13}C NMR spectrum of **SBF6.**

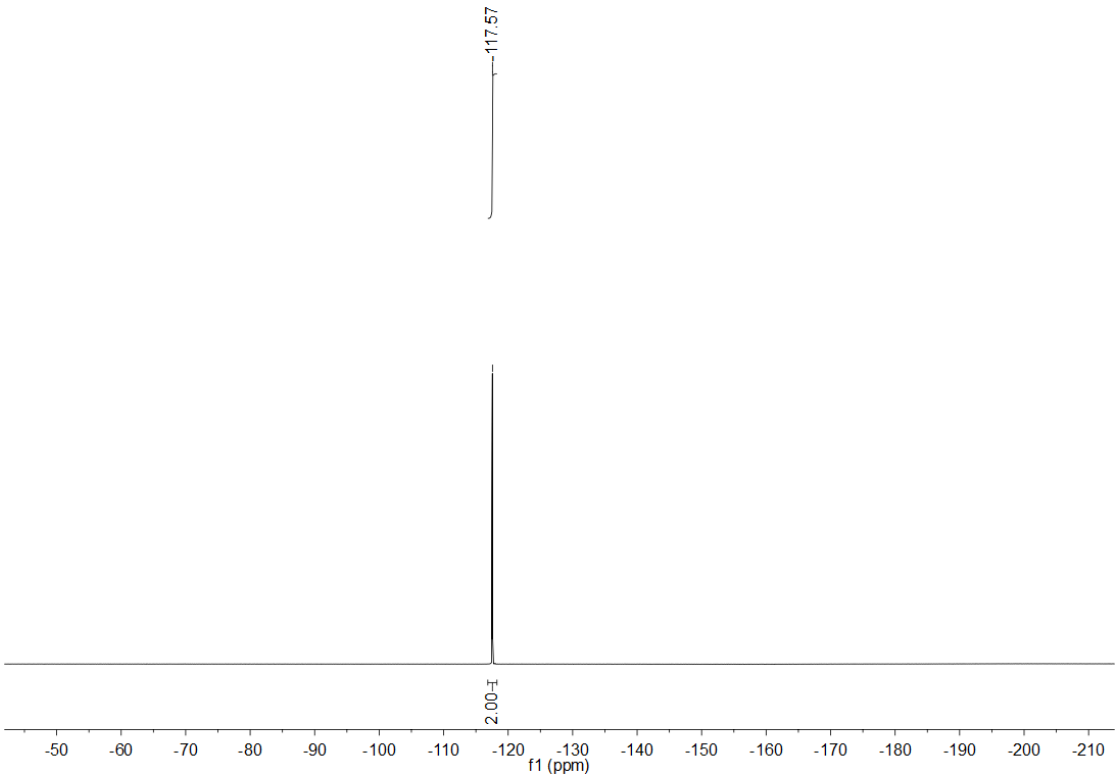

^{19}F NMR spectrum of **SBF6.**

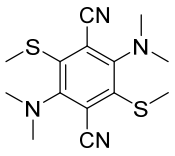

SBF7

^{1}H NMR spectrum of **SBF7.**

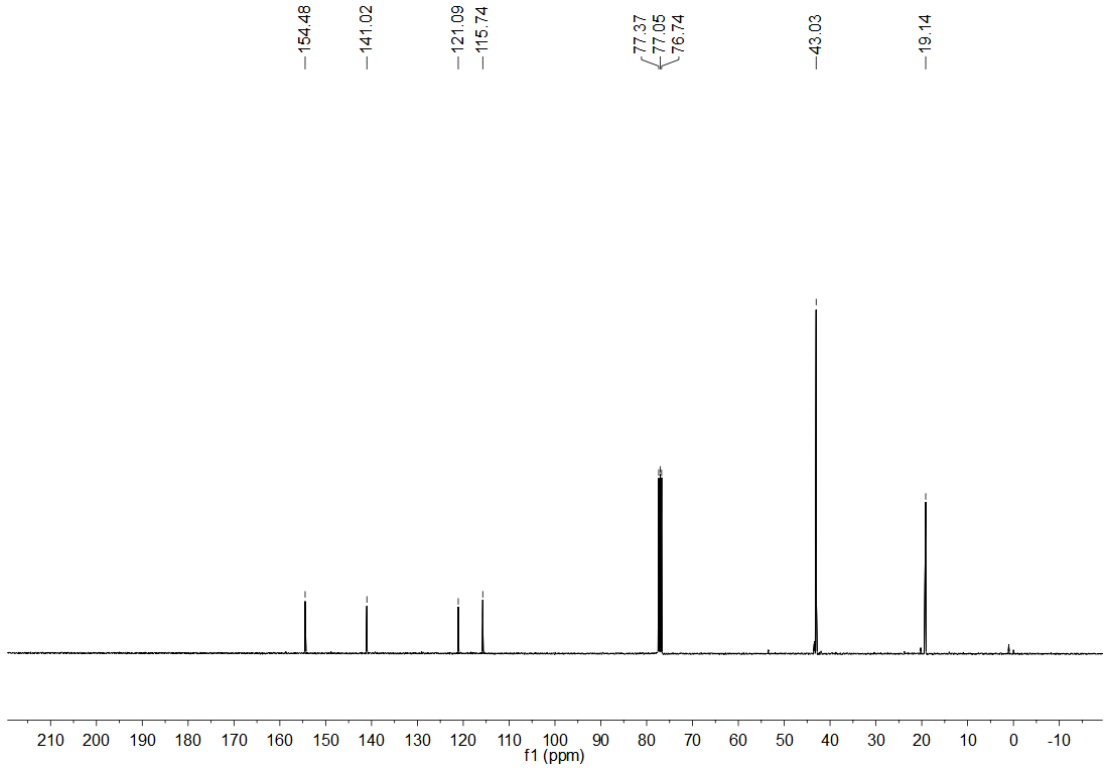

^{13}C NMR spectrum of **SBF7.**

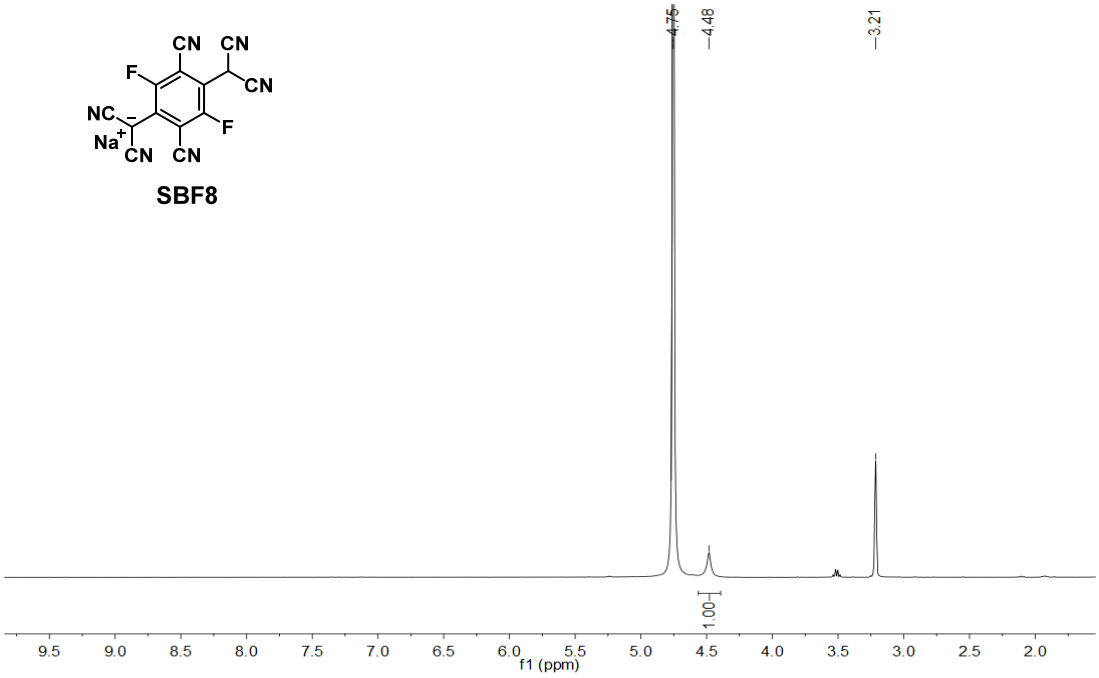

^{1}H NMR spectrum of **SBF8.**

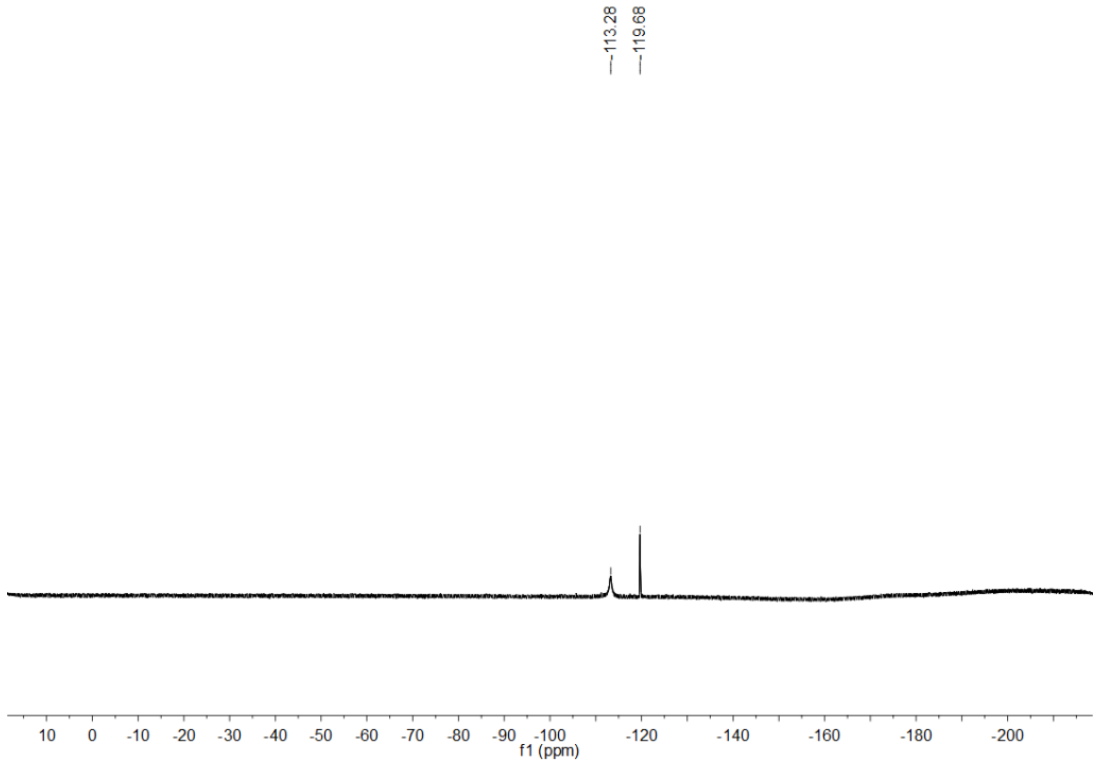

^{19}F NMR spectrum of **SBF8**

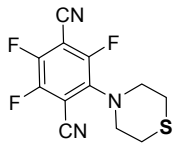

HClO-SBF

^{1}H NMR spectrum of **HClO-SBF.**

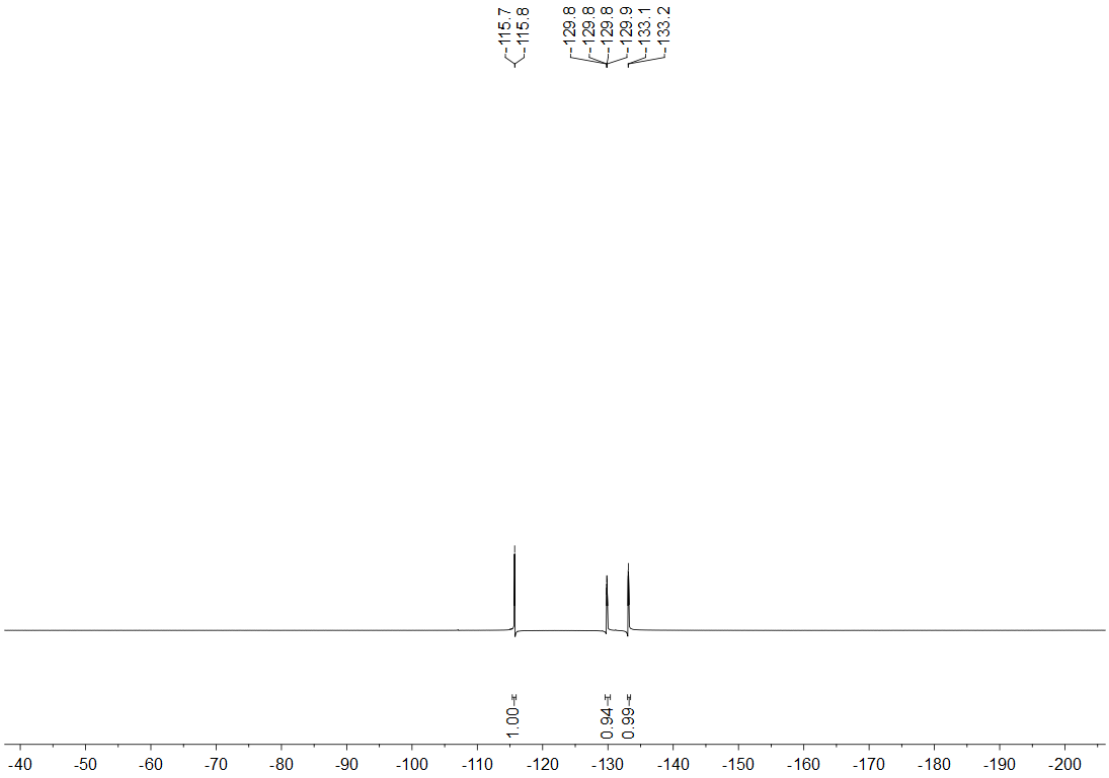

^{19}F NMR spectrum of **HClO-SBF.**

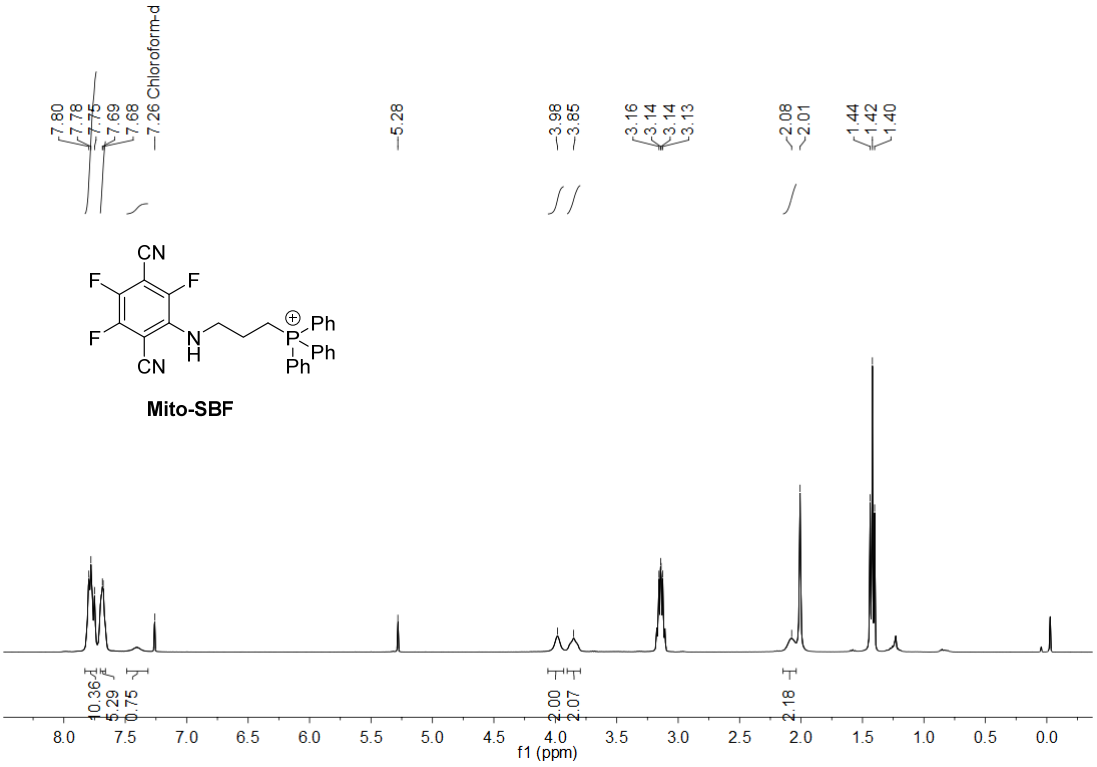

^{1}H NMR spectrum of **Mito-SBF.**

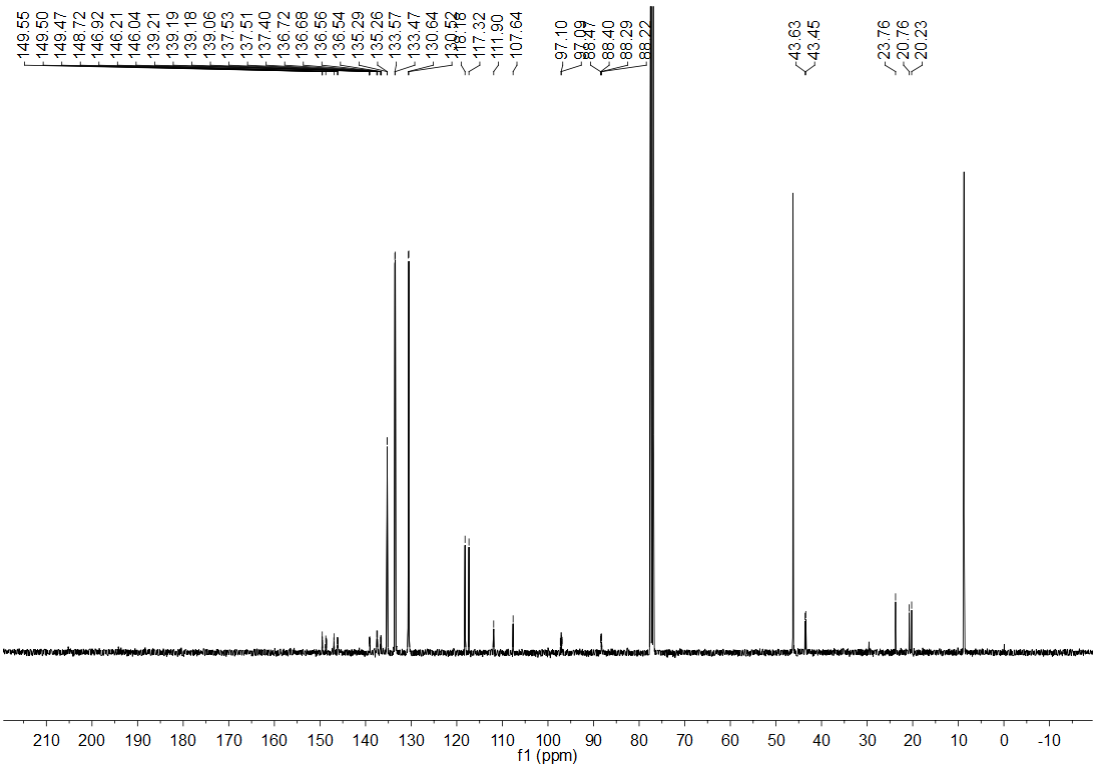

^{13}C NMR spectrum of **Mito-SBF.**

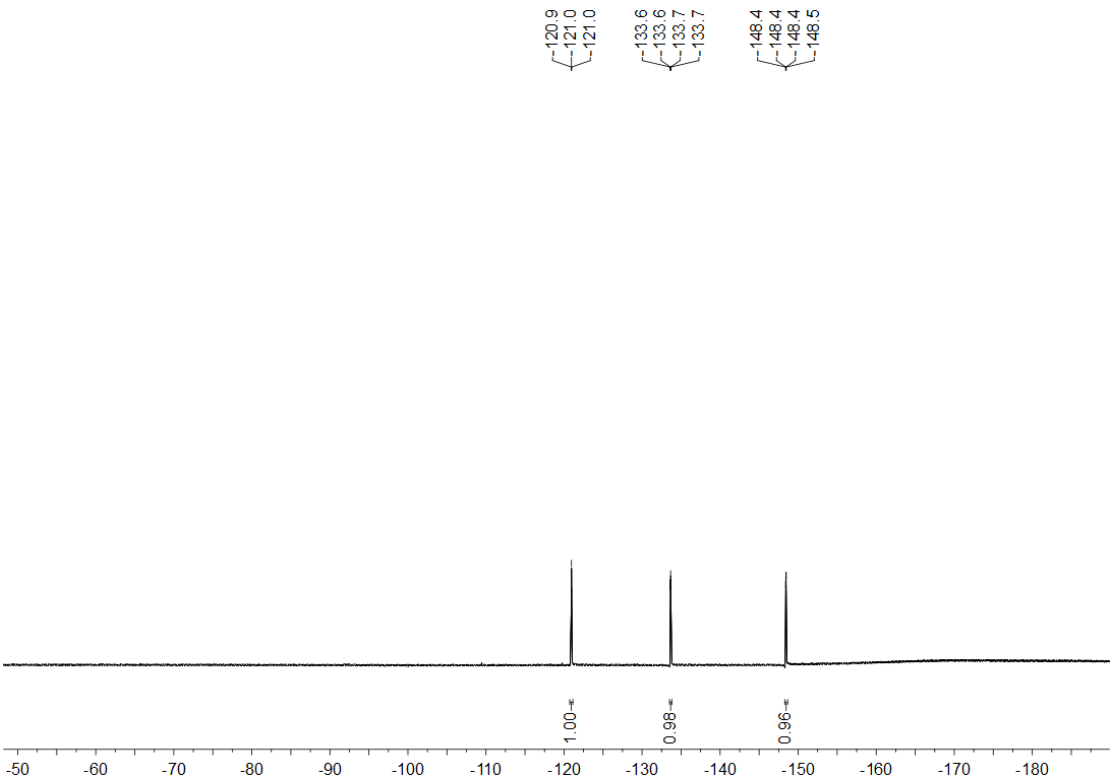

^{19}F NMR spectrum of **Mito-SBF.**

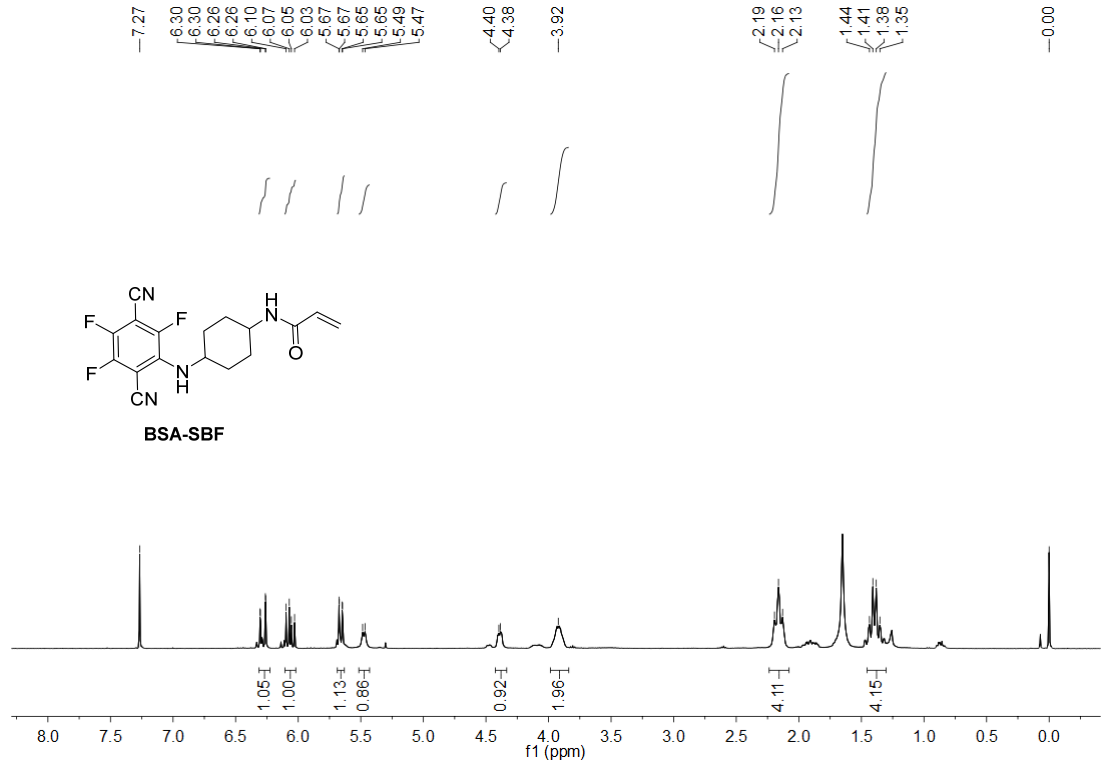

^{1}H NMR spectrum of **BSA-SBF.**

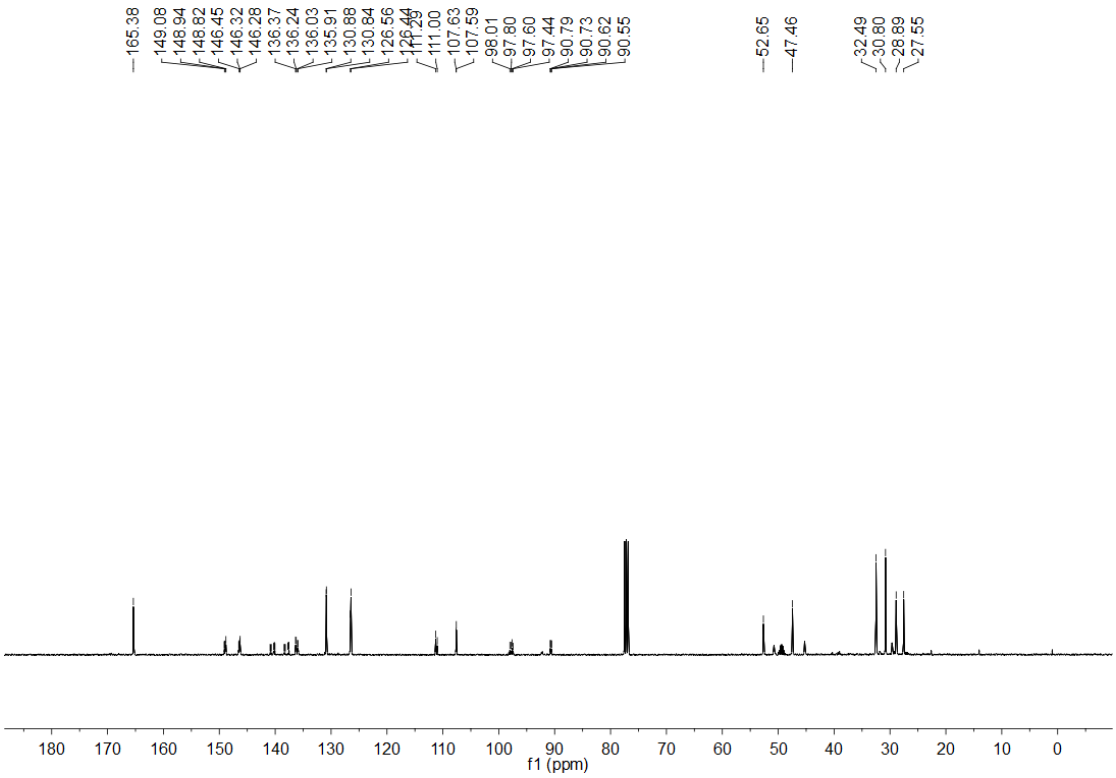

^{13}C NMR spectrum of **BSA-SBF.**

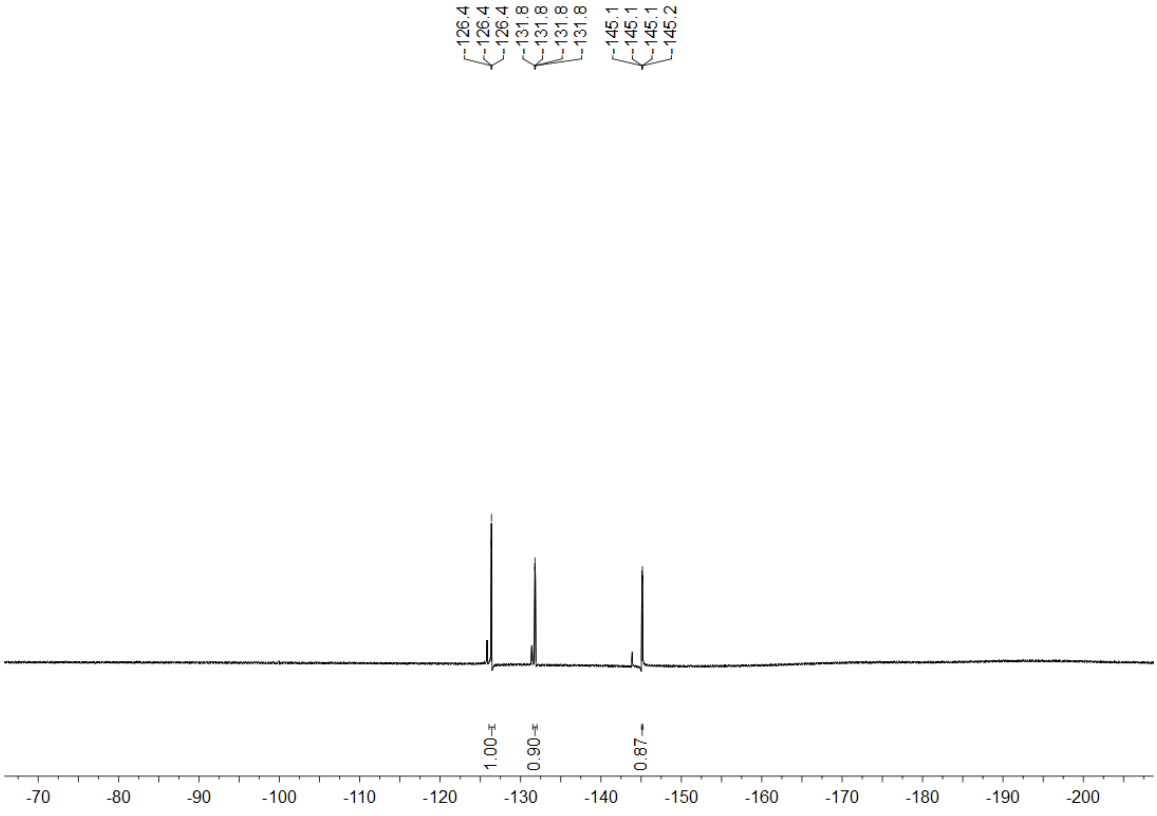

^{19}F NMR spectrum of **BSA-SBF.**

6 References:

(1) Melhuish ,W. H. Quantum Efficiencies of Fluorescence of Organic Substances: Effect of Solvent and Concentration of the Fluorescent Solute1. *J. Phys. Chem.* **1961**, *65*, 229-235.

(2) Kubin, R. F.; Fletcher, Fluorescence Quantum Yields of Some Rhodamine Dyes. *J. Lumin.* **1982**, *27*, 455-462.

(3) Rurack, K.; Spieles, M. Fluorescence Quantum Yields of a Series of Red and Near-Infrared Dyes Emitting at 600−1000 nm. *Anal. Chem.* **2011**, *83*, 1232-1242.

(4) Makarov, N. S.; Drobizhev, M.; Rebane, A. Two-photon Absorption Standards in the 550–1600 nm Excitation Wavelength Range. *Opt. Exp.* **2008***, 16,* 4029-4047.